Glasses and Glass-Ceramics for Nuclear Waste Immobilization

D. Caurant, Odile Majérus

Caurant, Daniel and Majérus, Odile (2021) Glasses and Glass-Ceramics for Nuclear Waste Immobilization. In: Pomeroy, M. (ed) Encyclopedia of Materials: Technical Ceramics and Glasses, vol. 2, pp. 762–790. Oxford: Elsevier. https://doi.org/10.1016/B978-0-12-818542-1.00090-4

Glasses and glass-ceramics for nuclear waste immobilization

Daniel Caurant and Odile Majérus

Chimie ParisTech, PSL Research University, CNRS, Institut de Recherche de Chimie Paris (IRCP), UMR 8247, 75005 Paris, France

Email address: daniel.caurant@chimieparistech.psl.eu; odile.majerus@chimieparistech.psl.eu

Introduction

As all other industries and human activities, nuclear industry generates waste during energy production (electricity) or weapons fabrication. However, in the case of nuclear industry some of these waste are highly radioactive and must be isolated durably from the biosphere in highly durable matrices for several thousands of years or more in order to limit their potential impact on the environment (Jantzen C. M., Brown K. G. and Pickett J. B. 2011, Vernaz E., Gin S. and Veyer C. 2012, Pegg I. L. 2015). This is different from the case of certain types of non-nuclear hazardous industrial or domestic waste that can be recycled to make useful materials (glasses, glass-ceramics) that severely limit the rate of release of toxic elements (heavy metals) in the environment (Colombo P., Brusatin G., Bernardo E. and Scarinci G. 2003, Donald I. W. 2007 and 2016).

In commercial nuclear power reactors, the burn up of ^{235}U enriched UO_2 fuel under thermal neutrons produces energy due to the fission of uranium nuclei and generates a wide spectrum of fission products (Table 1), and actinides by neutrons capture (plutonium and other actinides).

Chemical family	Weight (kg/U)
Rare gases (Kr, Xe)	5.6
Alkalis (Cs, Rb)	3
Alkaline-earths (Sr, Ba)	2.4
Rare earths (Y, lanthanides)	10.2
Transition metals (Mo, Zr, Tc)	7.7
Chalcogens (Se, Te)	0.5
Halogens (I, Br)	0.2
Noble metals (Ru, Rh, Pd)	3.9
Others (Ag, Cd, Sn, Sb…)	0.1

Table 1. Main families of fission products occurring in spent nuclear fuel before reprocessing. The values given in this table correspond to that of a UO_2 spent fuel enriched with 3.5% ^{235}U (burn-up 33 GWday.t^{-1} in a pressurized

water reactor, 3 years after discharge) given in kg by ton of U before burning. It can be remarked that rare earths (Y + lanthanides) constitute the most abundant family of fission products in wt%. More than 300 radionuclides (β, γ emitters) are produced during fuel burn-up but more than 60% of them will have disappeared several times after spent fuel discharge. Nearly 40 elements of the Mendeleyev classification from Ge to Dy are generated during fission reactions. (Boullis and Devezeaux de Lavergne 2006).

Several countries such as the US, Canada and Sweden decided not to reprocess their spent nuclear fuel leaving it in interim storage while waiting for possible disposal (open fuel cycle), whereas for several decades other countries such as France, Russia, the UK and Japan reprocessed their spent nuclear fuel to recover remaining uranium and plutonium to prepare new nuclear fuel (MOX fuel, mixed oxide fuel consisting of Pu mixed with natural uranium, reprocessed uranium, or depleted uranium) and also to reduce the radiotoxicity of the ultimate waste containing the fission products and minor actinides (closed fuel cycle) (Wilson P. D. 1996, Rodríguez-Penalonga L. and Moratilla Soria B. Y. 2017). Indeed, spent nuclear fuel may still contain about 96 wt% of reusable material (U + Pu) to produce energy**.** The ultimate high level radioactive waste (HLW) recovered after the reprocessing of spent nuclear fuel coming from energy production (commercial waste) and also the ones coming from plutonium weapons fabrication referred as to defense waste (Metcalfe B. L. and Donald I. W. 2013) are today conditioned by dissolution at the atomic scale in highly durable glassy or partially crystallized matrices (Ojovan M. I. and Lee W. E. 2007, Caurant D., Loiseau P., Majérus O., Aubin-Chevaldonnet V., Bardez I. et al. 2009, Jantzen C. M. 2011, Vernaz E., Gin S. and Veyer C. 2012, Donald I. W. 2016, Jantzen, C. M. and Ojovan, M. I. 2019). In these wasteforms, the glassy and crystalline phases play the role of solvent for almost all the species - radioactive or not - initially present in the waste (Fig. 1). Several other nuclear waste generally less radioactive (low or intermediate radioactive level waste) than the reprocessing waste originating for instance from nuclear installations dismantling or other sources could also be immobilized in glassy matrices (Sobolev I. A., Dimitriev S. A., Lifanov F. A., Kobelev A. P., Stefanovky et al. 2005, Cantrel E., Courtadon A., Blanchard S. and Girold C. 2015, Girold C., Francois S., Petit L., Catherin S., Prevost T. et al. 2018).

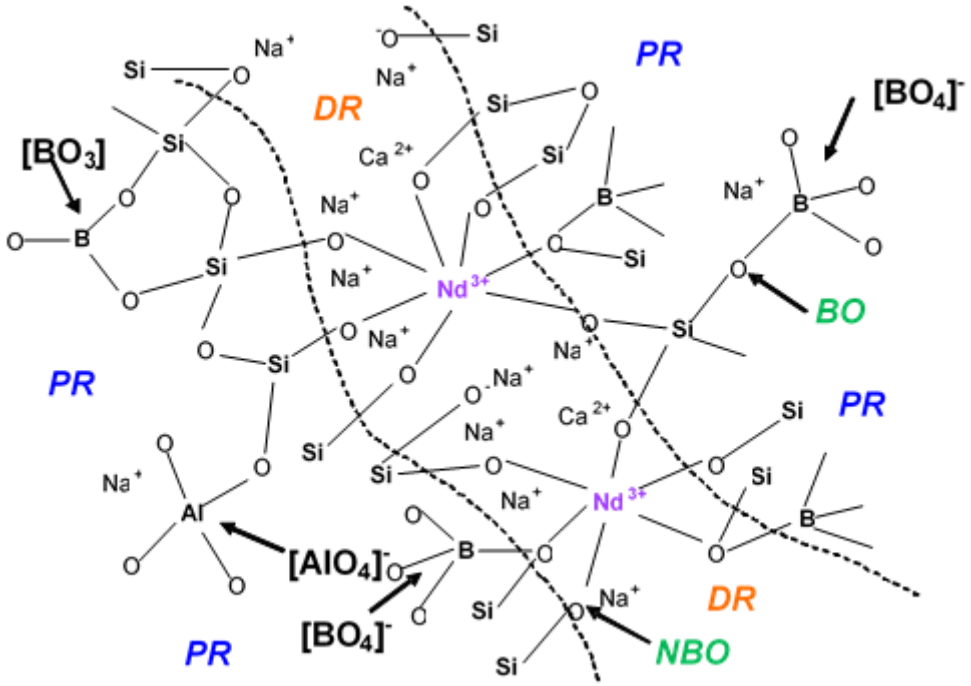

Figure 1. Structural scheme showing the way fission products such as neodymium (one of the most abundant lanthanides present in HLW, Fig. 3) may enter into the structure of a peralkaline borosilicate nuclear glass. Nd^{3+} ions may be located in the depolymerized regions (DR) of the glass structure that are rich in non-bridging oxygen atoms (NBOs) and alkali + alkaline-earth cations (here Na^+ and Ca^{2+}). In these regions, NdO_n polyhedra can be locally charge compensated by alkali + alkaline-earth cations. Polymerized regions (PR) rich in bridging oxygen atoms (BOs) are also shown.

In this Chapter, after considering the nature and composition of HLW, and the specifications of an efficient wasteform to incorporate these waste, the focus will be on the vitrification processes performed by melting the mixture of a glass frit with waste, and on the way several problematic elements present in the waste such as cesium, technetium, molybdenum, zirconium, lanthanides and actinides can be incorporated in the structure of glasses (such radioactive wasteforms are generally called nuclear glasses or nuclear waste glasses). The effect of glass composition changes on the incorporation of some of these elements (solubilization, demixing in the melt, crystallization) will also be considered by focusing on alkali-lime aluminoborosilicate type wasteforms that represent the main type of nuclear glasses used worldwide for HLW containment. The case of waste incorporation in glass-ceramics that can be envisaged to immobilize non-separated HLW or separated long-lived radionuclides will also be developed. After an interim storage period, all these conditioned waste will have to be kept by geological disposal in a deep underground repository following a multiple barrier containment approach (Ewing R. C., Whittleston R. A. and Yardley B. W. D. 2016, Grambow B. 2016, Laverov N. P., Yudintsev S. V., Kochkin B. T. and Malkovsky V. I. 2016) where the glassy or partially

crystallized wasteforms will constitute the first containment barrier. The long-term behavior against water alteration and self-irradiation of nuclear glasses will also be addressed.

Nature of highly radioactive waste and need for their immobilization

HLW generally contain high amounts of α, β and γ radionuclides which are particularly harmful to the living world, even if radioactivity also exists in nature (^{235}U, ^{238}U, ^{232}Th, ^{40}K). They are produced in nuclear reactors, the aim of which is to produce electricity or plutonium for military purposes. In both cases, nuclear fuel is subjected to a neutron flux leading to the production of energy (and then electricity for power reactors) and the formation of fission products (FP, Table 1) and minor actinides (MA: Np, Am, Cm) generated by neutrons capture mainly by ^{238}U (as for Pu formation) that constitute very dangerous (highly radioactive and toxic) non-reusable ultimate wastes. These wastes represent only around 4 wt% (comprising mainly FP and 0.1 wt% MA) of the spent fuel for power reactors.

In the context of nuclear weapons, spent fuel is reprocessed by dissolution in acid solutions to recover plutonium (Metcalfe B. L. and Donald I. W. 2013). Civilian spent fuel can be reprocessed in the same way (Purex process), in order to recover the uranium and plutonium remaining in the spent fuel (about 96 wt%) to prepare new nuclear fuel (Wilson P. D. 1996, Bonin B. 2008, Nuclear Energy Agency 2018). In both cases, the remaining ultimate HLW that are present as concentrated aqueous nitric solutions are stored during more or less long periods in metallic tanks to enable a significant decrease of their radioactivity and thermal power before conditioning. Depending on the type of nuclear reactor, fuel and cladding nature, on the fuel composition and burn-up, and on the particularities of the extraction processes, the composition of HLW may strongly vary between countries and within the same country over time. For instance, the concentrations of FP are relatively low in the HLW solutions originating from the reprocessing of defense spent fuels or civilian spent fuels using natural uranium (0.7% ^{235}U) because of their low burn-up in comparison with the HLW solutions originating from pressurized water reactors (PWR) using ^{235}U-enriched fuel (Donald I. W., Metcalfe B. L. and Taylor R. N. J. 1997, Donald I. W. 2016), because the amount of FP increases proportionally with the burn-up of the fuel. As they contain long-lived α and β radionuclides for which half-lives can reach thousands to millions of years (MA, ^{135}Cs, ^{99}Tc, ^{93}Zr…), HLW must be isolated from the biosphere from thousands to hundreds of thousands of years, at least until their radiotoxicity level drops back to the radiotoxicity level of the initial uranium ore (Fig. 2).

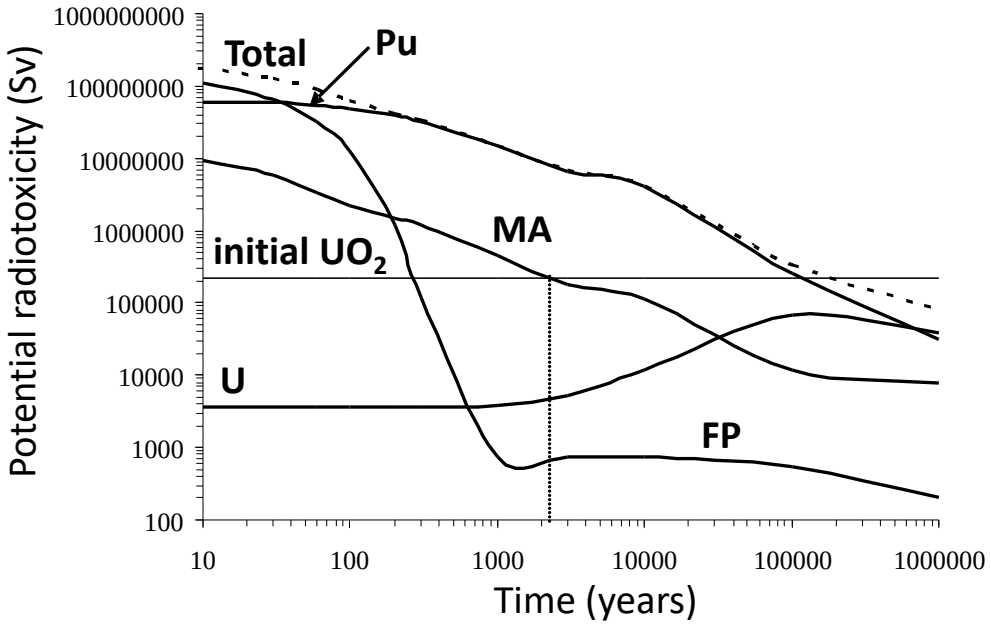

Figure 2. Evolution with time of the potential radiotoxicity (expressed in Sv/ton of initial uranium metal) of a UO_2 enriched spent fuel with 3.5 % of ^{235}U from a power reactor (burn-up 33 GWday.t^{-1} and 3 years after discharge) showing the contribution of plutonium, uranium, minor actinides (MA) and fission products (FP). The level of radiotoxicity of the initial natural uranium ore (UO_2) taking into account ^{235}U enrichment is indicated for comparison (horizontal line). The vertical dotted line indicates the time needed for MA to reach a radiotoxicity level close to that of the initial ^{235}U-enriched fuel. It clearly appears that after plutonium extraction from the waste (reprocessing), the most problematic long-term radionuclides are MA. After reprocessing (Pu and U extraction), the main contribution to the potential radiotoxicity will be due (during 2-3 centuries) to the short-lived β-emitters such ^{137}Cs and ^{90}Sr (FP) and then to the long-lived α-emitters such as ^{241}Am, ^{243}Am and ^{244}Cm (MA). (Modified from Bardez I. (2004) Study of the structural characteristics and properties of glasses rich in rare earths intended for the immobilization of fission products and long-lived elements (in French). PhD of the University Pierre and Marie Curie. Paris, France. https://pastel.archives-ouvertes.fr/pastel-00001075; p.10).

Immobilization of highly radioactive nuclear waste

HLW solutions originating from spent nuclear fuel reprocessing contain FP, MA and also additional non-radioactive but relatively abundant elements coming from the Purex process (P, Na) and from the corrosion of the tanks (Fe, Ni, Cr) in which are kept HLW solutions (Fig. 3). Because of the risks of diffusion and dispersion of these waste in the biosphere and also to facilitate their transport and storage, they must be conditioned in solid and highly durable matrices before deep underground disposal. Nowadays, all the elements present in HLW solutions are immobilized together in a same matrix, but numerous studies have been carried out in order to selectively extract from these solutions the most active and long-lived α or β radionuclides such as MA and Cs (^{135}Cs half-life of 2.3 million years) using enhanced

reprocessing processes with appropriate extracting molecules (Madic C. Lecomte M., Baron P. and Boullis B. 2002, Bonin B. 2008) and then to find specific very durable wasteforms for these separated radionuclides (Caurant D., Loiseau P., Majérus O., Aubin-Chevaldonnet V., Bardez I. et al. 2009). For instance, many works have been carried out on highly durable ceramic (zirconates, phosphates, titanates) and also on glass-ceramic matrices for the specific immobilization of MA (Guy C., Audubert F., Lartigue J-E., Latrille C., Advocat T. et al. 2002, Caurant D., Loiseau P., Majérus O., Aubin-Chevaldonnet V., Bardez I. et al. 2009). Similar types of studies have also been conducted on ceramics, glasses and glass-ceramics for the immobilization of plutonium-rich waste (Muller I. and Weber W. J. 2001, Zhang Y., Gregg D. J., Kong L., Jovanovich M. and Triani G. 2017). The possibility to immobilize long-lived ^{129}I (half-life of 15.7 million years) in glassy and ceramic matrices has also been investigated, iodine being recovered separately during spent fuel dissolution in nitric solutions (Lemesle T., Méar F. O., Campayo L., Pinet O., Revel B. et al. 2014, Riley, B. J., Vienna, J. D., Strachan, D. M., McCloy, J. S. and Jerden, J. L. 2016, Yang J.H., Park H-S. and Cho Y-Z. 2017).

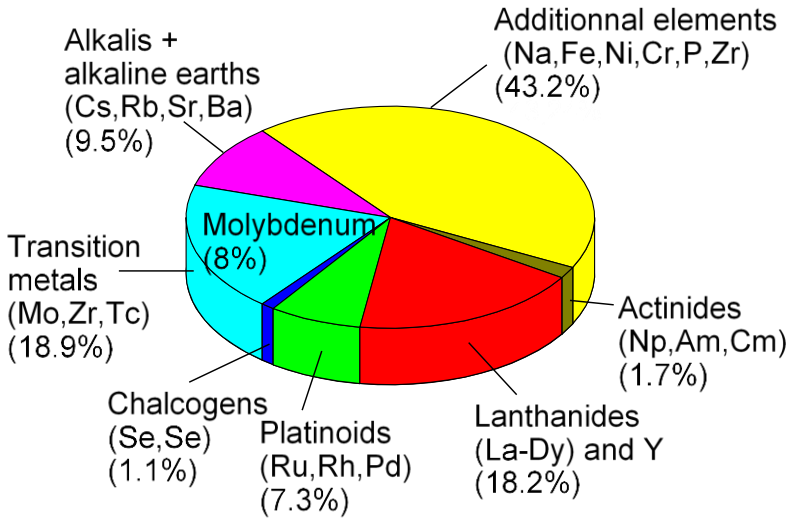

Figure 3. Relative abundance (in wt% of oxides) of the different families of elements present in HLW solutions originating from the reprocessing of an UO_2 enriched (3.5% ^{235}U) spent fuel (see details in the legend of Table 1).

Because of its low chemical durability, its high thermal power (due to the high concentration of thermal radionuclides) and its high specific area, the solid calcine that can be obtained after water evaporation and calcination of HLW solutions is not itself an efficient wasteform without the addition of other elements (such as Si, B, Al, alkalis and alkaline-earths for borosilicate glassy wasteforms). It can only be considered as an intermediate product that must be immobilized by dissolution or dispersion (by partial or total encapsulation) in a more durable

solid matrix. When looking for an efficient wasteform for HLW containment, several important points must be considered concerning both the properties of the final matrix and the difficulties that can be encountered for its synthesis in radioactive environment (Caurant D., Loiseau P., Majérus O., Aubin-Chevaldonnet V., Bardez I. et al. 2009, Jantzen, C. M. and Ojovan, M. I. 2019). For instance, concerning the properties of the matrix:

- The matrix must incorporate almost all the elements (radioactive or not) of the wastes with a sufficiently high loading to limit the volume of the wasteform (high incorporation capacity) while taking into account the heating generated by radionuclides disintegration - such as ^{137}Cs, ^{90}Sr, ^{241}Am and ^{244}Cm - that could affect matrix structure and microstructure and could be problematic for storage and disposal (increase of the minimum distance between canisters).
- The matrix must exhibit very good long-term behavior concerning both its resistance against alteration by water (liquid and vapor) and its resistance against self-irradiation. Even if structural evolution occurs specially under the effect of α-decays, the chemical durability and the capacity of the matrix to retain radionuclides must remain acceptable.

Concerning the synthesis of the wasteform:

- The process to incorporate the wastes into the matrix must be as simple as possible and the number of steps must be small in order to avoid the production of high amounts of secondary radioactive wastes and to reduce the cost of immobilization.
- The temperature of synthesis must not be too high to limit the risks of evaporation and to take into account furnaces and canisters limitation.

To meet these requirements, numerous kinds of glasses, glass-ceramics and crystalline (single phase or multiphase) matrices have been envisaged (Hench L. L., Clark D. E. and Harker A. B. 1986, Donald I. W., Metcalfe B. L. and Taylor R. N. J. 1997, Donald I. W. 2007, Lee W. E., Ojovan, M. I., Stennett M. C. and Hyatt N. C. 2006, Caurant D., Loiseau P., Majérus O., Aubin-Chevaldonnet V., Bardez I. et al. 2009, Jantzen, C. M. and Ojovan, M. I. 2019). Nevertheless, because of their ease of synthesis (melting + casting), their high loading capacity related to their structural flexibility and lack of stoichiometry facilitating waste incorporation, their very good self-irradiation resistance and good chemical durability, glassy matrices still represent today the main type of matrix implemented on an industrial scale since 1978 to immobilize HLW (Vernaz E., Gin S. and Veyer C. 2012, Ojovan M. I. and Lee W. E. 2010, Gin S., Jollivet P., Tribet M., Peuget S. and Schuller S. 2017). In glassy wasteforms the majority of the elements coming from HLW may adapt more easily than in crystalline phases their local environment according to their size, their ionic charge and the amount of non-bridging oxygen atoms (NBOs) and charge compensators available in glass composition (see Fig. 1 for Nd^{3+} ions incorporation in an

borosilicate glass). Nevertheless, many studies have been performed to develop matrices consisting of a glassy phase and one or more durable crystalline phases able to incorporate wastes in their structure and a current tendency is to accept partial crystallization in glassy matrices to reach higher waste loading, if it is not detrimental to the containment properties of the wasteform (Caurant D., Majérus O., Fadel E., Lenoir M., Gervais C. et al. 2007, Crum J. V., Turo L., Riley B, Tang M. and Kossoy A. 2012) (Fig. 4).

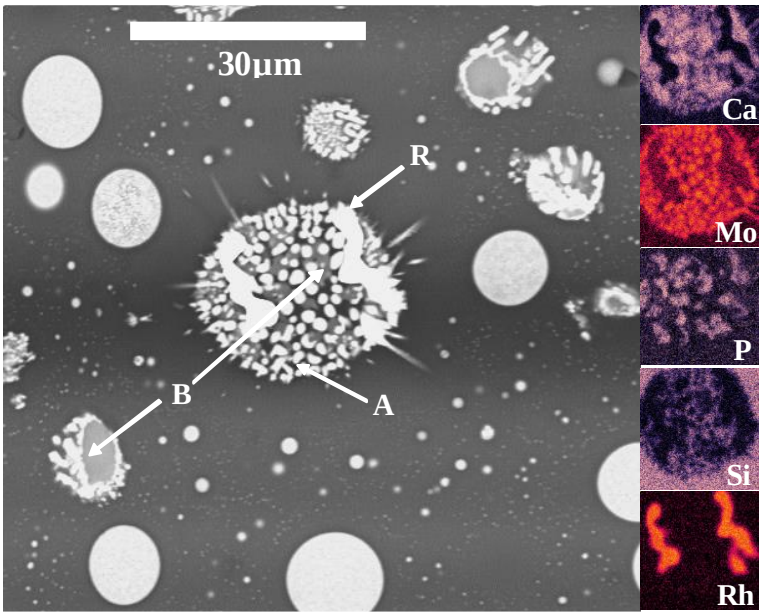

Figure 4. Back-scattered SEM image and EDX cartography of a partially crystallized borosilicate glass developed for the immobilization of Mo- and P-rich HLW waste. The EDX cartography shows the distribution of the elements in the big crystallized droplet located in the center of the image. **A**: white phase containing Ca and Mo ($CaMoO_4$); **B**: grey phase containing P and Ca ($NaCaPO_4$); **R**: white phase containing rhodium. (Caurant D., Majérus O., Fadel E., Lenoir M., Gervais C. and Pinet O. (2007) Effect of molybdenum on the structure and on the crystallization of SiO_2-Na_2O-CaO-B_2O_3 glasses. *J. Am. Ceram. Soc.* **90**, 774-783, p.775. Reproduced with permission from John Wiley and Sons)

In comparison with glassy wasteforms, due to their lower structural flexibility associated with long range order and their more complex preparation (grinding + pressing + sintering steps), single phase ceramic matrices are not well adapted to incorporate the wide spectrum of elements with different sizes and charges present in HLW solutions (Fig. 3). They are more adapted for the containment of specific radionuclides (MA, Pu, Cs) (Aubin-Chevaldonnet V., Caurant D., Dannoux A., Gourier D., Charpentier T. et al. 2007, Wang L. and Liang T. 2012, Orlova A. I. and Ojovan M. I. 2019). Indeed, the composition and the structure of such matrices must be selected according to the crystallographic sites available to immobilize the elements from the waste. Nevertheless, even if their synthesis appears more complex than that of glasses, multi-

phase ceramics such as the Synroc ceramics containing different highly durable crystalline phases each adapted to immobilize different groups of the elements present in HLW or in actinide-rich waste have been envisaged (Gregg D. J. and Vance E. R. 2016).

Vitrification of highly radioactive nuclear waste

Nowadays, HLW recovered from civilian and defense spent fuel reprocessing are incorporated by dissolution into the structure of borosilicate or aluminophosphate glasses melted in ceramic or metallic melters at temperature not exceeding 1100-1150°C and casted in metallic containers to obtain large glass blocks (~ 400 kg) before interim storage, using continuous melting processes industrialized since more than 40 years (Vernaz E., Gin S. and Veyer C. 2012). Because of the lack of sufficient glass formers, fluxing agents and charge compensators in HLW composition (Fig. 3), it is necessary during melting to add to the waste a high proportion (~ 70-80 wt%) of a glass frit (supplied by a glassmaker) to provide the glass former (SiO_2, B_2O_3, P_2O_5), intermediate (Al_2O_3) and modifier (Na_2O, Li_2O, CaO) oxides necessary to form the glassy network (Fig. 1) and to enable the dissolution in this structure of the elements coming from the waste (Fig. 5).

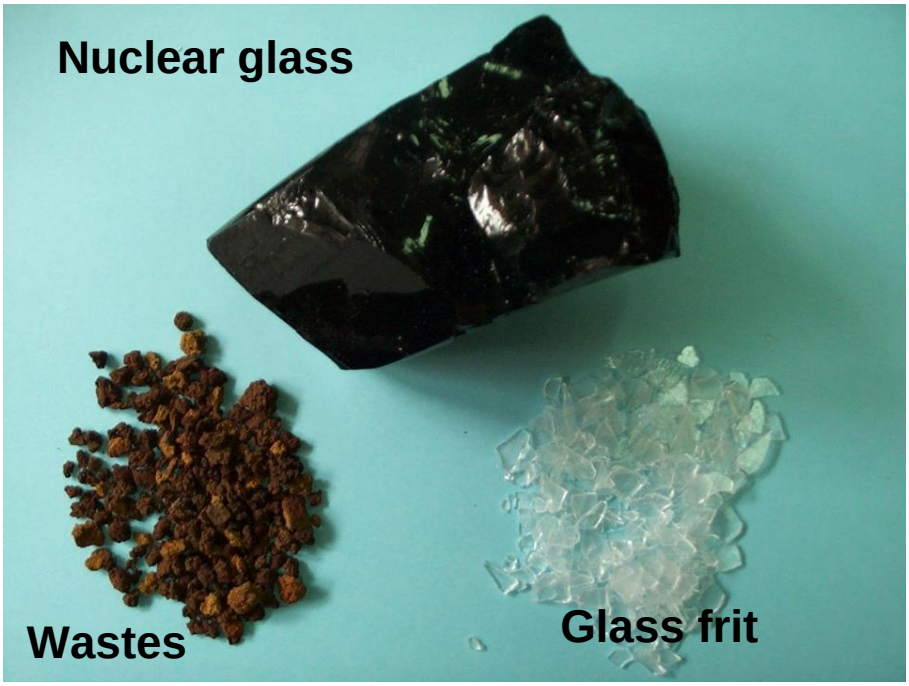

Figure 5. Example of a borosilicate glass frit (right), calcined inactive waste (left) and inactive nuclear borosilicate glass (top) that can be synthesized at lab-scale to test glass frit formulation. Because of the high amounts of elements present in the waste that absorb in the visible domain (transition metals, lanthanides), the glass has a black color.

Using a pre-prepared glass frit to mix with the waste rather than a mixture of raw materials (oxides, carbonates…) as classically done in commercial glass industry enables to obtain more rapidly during heating a high amount of melt able to dissolve the waste. Moreover, this also avoids the generation in a radioactive environment of gases such as CO_2 coming from the raw materials. The choice of the composition of the glass frit results from a compromise between its incorporation capacity and its reactivity with the waste during melting which limits the waste loading (~ 18-35 wt%), the properties of the melt (viscosity) and its low liquid-liquid phase separation and crystallization tendency during cooling in the canister (the cooling rate is close to 1°C/min in the bulk of glass blocks), and the properties of the final wasteform (long-term behavior) as explained above. For instance, the crystallization of poorly durable phases likely to incorporate radionuclides or of SiO_2 and Al_2O_3-rich phases such as nepheline ($NaAlSiO_4$) that removes glass forming elements from the glass matrix and would induce a decrease of its chemical durability is usually avoided (Kim D.S., Peeler D.K. and Hrma P. 1995). Another issue due to crystallization could be the formation of cracks in the glass that can be due to the difference of thermal expansion coefficient between the crystals and the glass or to the incorporation of actinides in big size crystals (Chouard N., Caurant D., Majérus O., Dussossoy J.-L., Loiseau P. et al. 2019). The melt viscosity must be around 10 Pa.s both to enable a good melt homogenization (waste dissolution rate) and fining, to limit the evaporation of volatile elements and to enable melt casting in canisters. As classical soda-lime silicate melts exhibit a viscosity close to 10^3 Pa.s at 1100°C they are not suitable for waste vitrification in comparison with borosilicate and aluminophosphate melts which are much less viscous. As during industrial nuclear production waste composition variations may occur, it is also necessary that the glass frit formula must be flexible enough to keep acceptable wasteform properties (Vernaz E., Gin S. and Veyer C. 2012). To reach a final glass frit formulation numerous laboratory scale and pilot unit tests using simulated inactive waste, followed by tests with radioactive waste in a hot laboratory are required (Jantzen C. M. 2011, Vernaz E., Gin S. and Veyer C. 2012). In simulated inactive waste the radioactive elements (^{137}Cs, ^{90}Sr…) can be replaced by stable natural isotopes (^{133}Cs, ^{88}Sr…) whenever possible or using inactive surrogates exhibiting close chemical properties, for instance lanthanides to substitute actinides and rhenium to substitute technetium. The first tentative to use glass as nuclear wasteform was investigated in Canada in the 1950s (Lutze W. 1988), but the first industrial plant to produce borosilicate nuclear glasses only started in 1978 in France, using a metallic melter (Sombret C. G. 1993). Since this date, several industrial vitrification plants have been developed over the world to immobilize civilian or defense HLW using either ceramic or metallic melters (Ojovan M. I., Lee W. E. 2005, Jantzen

C. M., Brown K. G. and Pickett J. B. 2011, Pegg I. L. 2015, Donald I. W. 2016). Metallic melters used in France and in the UK are made of refractory metallic Ni-Cr-rich alloys in which the melt is heated indirectly by induction from the furnace wall and HLW solutions are calcinated before injection simultaneously with a glass frit in the furnace (Fig. 6) (Sombret C. G. 1993, Harisson M. T. 2014), while ceramic melters used for instance in the US, Russia, Japan and China are made of refractory ceramic blocks in which the melt is heated directly by Joule effect by means of submerged electrodes whereas HLW can be injected as slurry directly in the furnace (Jantzen C. M. 2011). A more recent alternative melting technique referred as to cold crucible induction process enabling to directly heat the melt by induction is employed in particular in France and in Russia (Sobolev I. A., Dimitriev S. A., Lifanov F. A., Kobelev A. P., Stefanovky S. et al. 2005, Vernaz E., Gin S. and Veyer C. 2012, Stefanovsky S. V., Lebedev V. V., Ptashkin A. G., Dmitriev S. A. and Marra J. C. 2010).

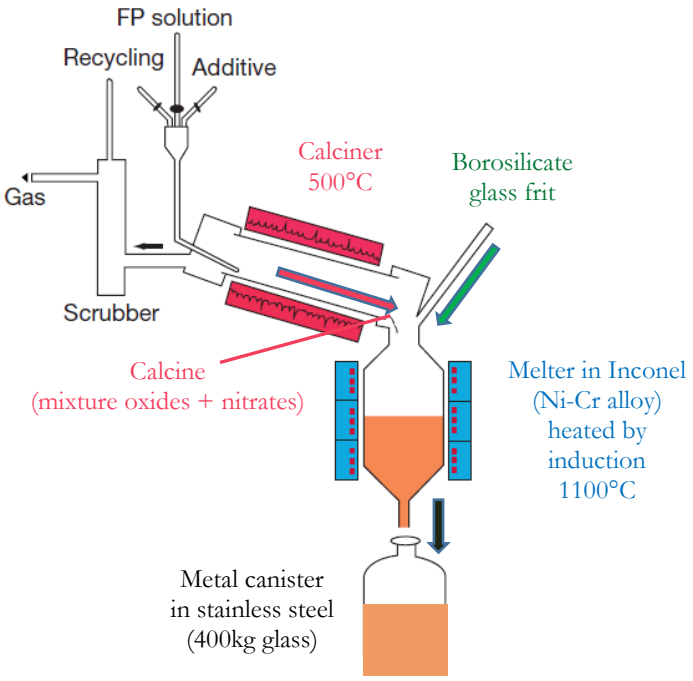

Figure 6. Scheme of the metallic melter used in France at the La Hague plant to immobilize commercial HLW in borosilicate glasses (glass production capacity ~ 25 $kg.h^{-1}$). In this two-step vitrification process, liquid waste solutions are firstly evaporated and calcined in a rotating furnace (in red). Melt stirring in the furnace enables the presence of significant amounts of insoluble noble metals by limiting the sedimentation risks. (Modified from Vernaz E., Gin S. and Veyer. C. (2012) Waste glass. *Comprehensive Nuclear Materials* **5**, 451-483. p. 475 with permission from Elsevier)

Usually, in all cases, the melt must be as homogeneous as possible in the furnace in order to limit the problems that could be induced by the settling of particles (clogging, short-circuits) and to reduce the presence of heterogeneities in the glass. However, melt stirring allows to

process melts with significant amounts of insoluble particles such as noble metals. The glass frit composition and waste loading are usually chosen to avoid as much as possible important crystallization and liquid-liquid phase separation during melting and cooling in canisters. Nevertheless, whatever the glass frit composition, the noble metals coming from HLW (Table 1) are almost insoluble in the melt (solubility ~100 ppm) and are present as micrometric crystalline heterogeneities in glasses (RuO_2, Pd, Rh, Pd-Te alloy) (Fig. 4). They represent only a weak fraction in the glass (<1 vol%), but their presence in the melt increases its viscosity and affects its electrical conductivity (Pflieger R., Malki M., Guari Y., Larionova J. and Grandjean A. 2009), and during cooling they may act as nucleation sites for heterogeneous crystallization (Pacaud F., Fillet C. and Jacquet-Francillon N. 1991, Orlhac X., Fillet C. and Phalippou J. 1999, Chouard N, Caurant D., Majérus O., Dussossoy J. L., Klimin S. et al. 2015). Classically, at laboratory scale or full-scale, tests are carried out on inactive compositions to evaluate the melt crystallization and phase separation tendency by studying the nature and the amounts of crystals or separated phases formed either after casting (to check melt homogeneity) or after isothermal treatments between the melting temperature and the glass transition temperature (T_g), or after controlled cooling from the melt (Orlhac, Fillet and Phalippou 1999, Rose, Woodward, Ojovan et al. 2011, Chouard N., Caurant D., Majérus O., Guezi-Hasni N., Dussossoy J.-L. et al. 2016) (Fig. 7).

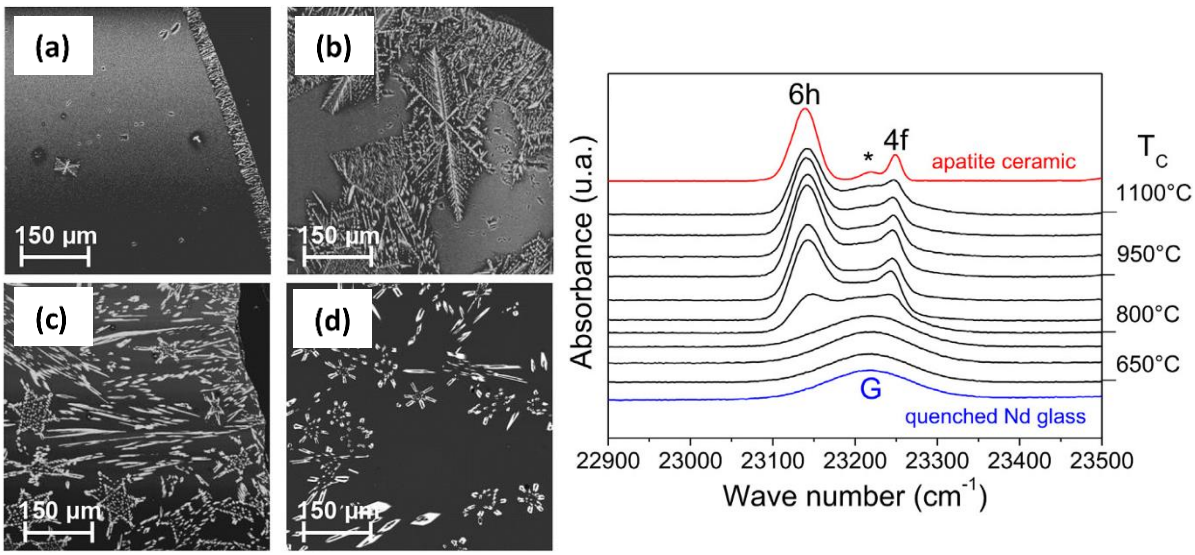

Figure 7. (left) Back-scattered electrons SEM images showing surface and bulk crystallization of $Ca_2Nd_8(SiO_4)_6O_2$ (apatite) crystals in a heat treated Nd_2O_3-rich inactive nuclear borosilicate glass heat treated 6h at T_c: (a) 750°C, (b) 800°C, (c) 950°C, (d) 1050°C. (right) Evolution of the Nd^{3+} optical absorption spectrum with the heat treatment temperature T_c showing the progressive incorporation of Nd^{3+} from the glass to the 6h and 4f sites of apatite crystals. (Chouard N., Caurant D., Majérus O., Guezi-Hasni N., Dussossoy J.-L., Baddour-Hadjean R. and Pereira-

Ramos J-P. (2016) Thermal stability of SiO_2-B_2O_3-Al_2O_3-Na_2O-CaO glasses with high Nd_2O_3 and MoO_3 concentrations. *J. Alloy. Compd.* **671**, 84-99; p. 89 and 93. Reproduced with permission from Elsevier)

In order to avoid any risk of crystallization during the interim storage and geological disposal, the glass temperature in canisters (due to radioactivity) must always remain lower than T_g, where atomic diffusion is very weak. This limits waste loading or involves adapting glass composition to increase T_g. For instance, for the French R7T7 borosilicate nuclear glass with T_g ~ 510°C, the equilibrium temperature reached in glass bulk one day after melt casting in canisters is about 400°C (i.e. about 100°C below T_g) and then very slowly decreases (Fig. 8). The experimental crystallization studies and long-term simulations performed on this glass confirmed that the main crystalline phases ($CaMoO_4$, $ZnCr_2O_4$, CeO_2) that may form could only grow at the beginning of melt cooling above T_g (Fig. 8). For instance, it was estimated by simulation that the time required to reach the total crystallization of CeO_2 and $ZnCr_2O_4$ phases in this glass (without considering the presence of platinoid heterogeneities) would be respectively 10^{28} and 57.10^3 years at 690°C (i.e. well above T_g) (Orlhac X. 1999).

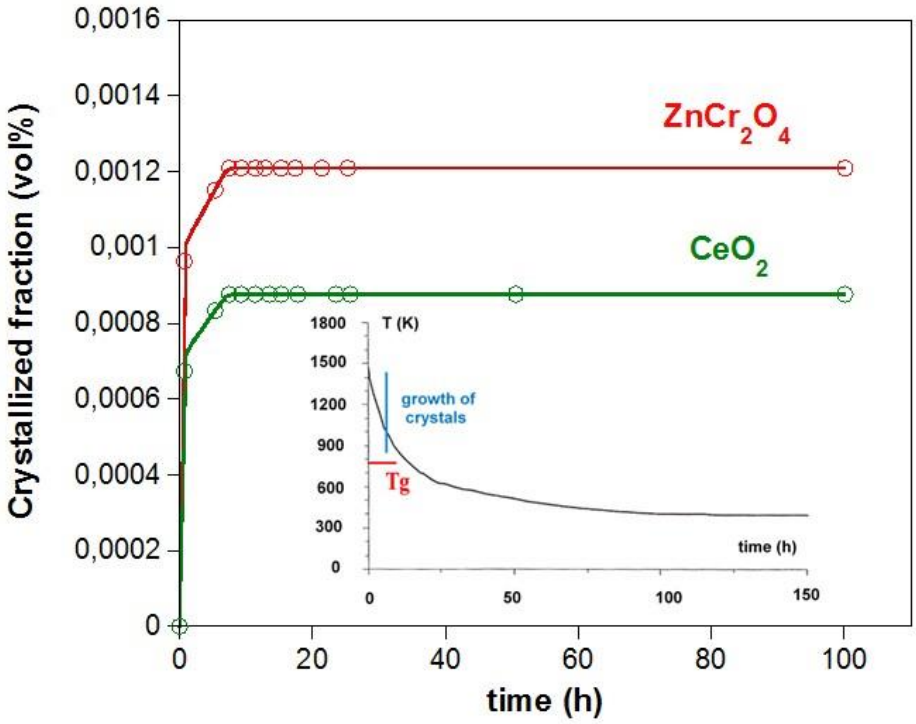

Figure 8. Modelisation of the evolution of the crystallized fraction (in vol%) of $ZnCr_2O_4$ and CeO_2 formed during cooling in the bulk of the R7T7 glass as a function of the time after melt casting in canister, following the bulk thermal evolution shown in the inset (natural cooling of a 400kg cylindrical glass block). The crystallized fractions were calculated from the nucleation and crystal growth rates of the two phases versus temperature. It appears that a very weak crystallization is only expected at the beginning of melt cooling. (Based on Orlhac X. (1999) Study

of the thermal stability of nuclear glass. Long-term evolution modeling. (In French) PhD of the University of Montpellier II (France). p. 179 and 180.
http://www.iaea.org/inis/collection/NCLCollectionStore/_Public/31/058/31058405.pdf)

Nuclear glasses structure and waste incorporation

Even if numerous works have been performed on various kinds of glass compositions such as iron phosphate and lead iron phosphate ones (Sales B. C. and Boatner L. A. 1986, Jantzen C. M. 2011, Bohre A., Avasthi K. and Pet'kov V. I. 2017), and lanthanide borosilicate ones (Meaker T. F., Peeler D. K., Marra J. C., Pareizs J. M. and Ramsey W. G. 1996, Jantzen C. M. 2011) to immobilize HLW, borosilicate glasses remain with aluminophosphate glasses (belonging to the P_2O_5-Al_2O_3-Na_2O system) the only kinds of glassy wasteforms produced industrially for HLW immobilization. However, because of their inferior chemical durability in aqueous environment and thermal stability, and the fact that their melts are more corrosive than borosilicate ones, aluminophosphate glasses are less used than borosilicate glasses (Bohre A., Avasthi K. and Pet'kov V. I. 2017). Nevertheless, aluminophosphate glasses can incorporate more easily in their structure higher amounts of molybdenum, actinides, lanthanides, sulfates and halides and thus appeared more adapted than borosilicate glasses to incorporate for instance Russian waste with high content of Al, Mo and sulfates (Laverov N. P., Yudintsev S. V., Kochkin B. T. and Malkovsky V. I. 2016).

To illustrate the chemical complexity of nuclear glasses used to immobilize HLW, the composition of the French R7T7 borosilicate nuclear glass is given in Table 2 and Fig 9 where SiO_2, B_2O_3, Al_2O_3, Na_2O, Li_2O, CaO and ZnO come from the glass frit and the other ones from HLW solutions (Fig. 3). In order to study at laboratory scale the structure, the thermal stability and the long-term behavior (chemical durability and self-irradiation effects) of such very complex borosilicate glasses, researchers preferentially used simplified and inactive compositions such as the International Simple Glass (ISG) one as reference glass which is a 6-oxide glass (SiO_2, B_2O_3, Al_2O_3, Na_2O, CaO, ZrO_2) considered as a good analogue of the R7T7 glass (Kaspar T. C., Ryan J. V., Pantano C. G., Rice J., Trivelpiece C. et al. 2019).

Oxide	wt%
SiO_2	45.6
B_2O_3	14.1
Na_2O	9.9
Al_2O_3	4.7
CaO	4.0
Fe_2O_3	1.1
NiO + Cr_2O_3	0.2
Li_2O	2.0
ZnO	2.5
P_2O_5	0.2
(FP + Zr) oxides + fines	16.4
actinide oxides	0.6

Table 2. Average composition of the French R7T7 nuclear borosilicate glass produced to immobilize HLW originating from the reprocessing of ^{235}U enriched UO_2 spent nuclear fuel with a waste loading of about 17 wt% (Vernaz, Gin and Veyer 2012). Fines suspension correspond to metallic particles present in HLW solutions generated during the fuel shearing operation. The inactive version of this glass, used for laboratory experiments, is referred as to SON68 glass.

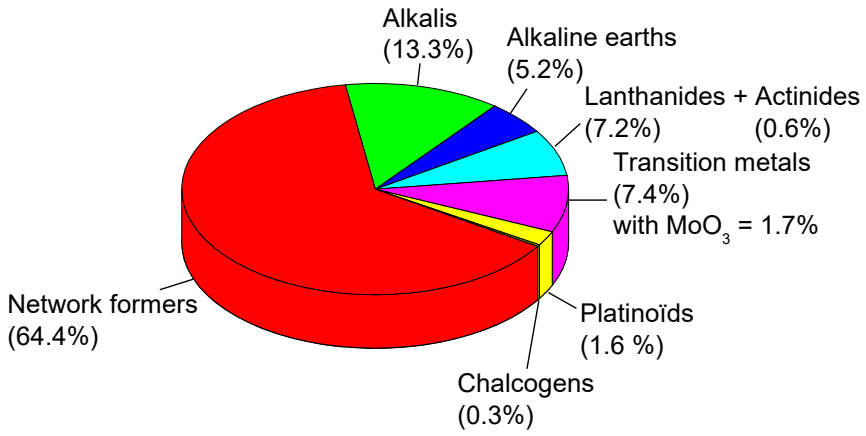

Figure 9. Relative abundance (wt%) of the different families of elements present in the R7T7 nuclear glass composition.

In such borosilicate nuclear glass compositions, the fact that the amount of SiO_2 (< 50 wt%) is significantly lower than in commercial soda-lime silicate glasses such as flat glass (> 70 wt%) and the presence of significant amounts of alkali oxides and B_2O_3 (close to 30 wt% in the R7T7 glass) enable to melt and cast them at relatively low temperature (1100-1150°C) in comparison with soda-lime silicate glasses (~1400-1500°C) because of the well-known fluxing and fluidizing effect of B_2O_3 and alkali oxides. Moreover, to limit the risks of matrix demixing

during melt cooling, the relative proportions of SiO_2, B_2O_3 and alkali oxides are chosen outside the phase separation region in the ternary SiO_2-B_2O_3-(Na_2O, Li_2O) phase diagrams (Jantzen C. M. 1986). Nevertheless, in order to maintain a good chemical durability against water alteration the proportion of B_2O_3 + alkali oxides must not be too high. As in borosilicate nuclear glasses there is generally an excess of alkali and alkaline-earth oxides compared to Al_2O_3 (such glasses are called peralkaline glasses), the glassy network is constituted of interconnected SiO_4, BO_4^-, BO_3 and AlO_4^- units with alkali and alkaline-earth cations charge compensating the BO_4^- and AlO_4^- units (Fig. 10), AlO_4^- units being preferentially charge compensated by alkali cations (Caurant D., Quintas A., Majérus O., Charpentier T. and Bardez I. 2008). The excess of alkali and alkaline-earth oxides of the glass frit forms NBOs on SiO_4 tetrahedra which enables to incorporate the majority of the wide spectrum of fission products and actinides that are present as cationic M^{n+} species in the waste, forming more or less strong M-O-Si bonds (see the Nd-O-Si bonds in Fig. 1). These alkali and alkaline-earth cations are not dispersed homogeneously in the glass structure but tend to form percolation channels in NBOs-rich regions (depolymerized regions in Fig. 1) (Le Losq G., Neuville D. R., Chen W., Florian P., Massiot D. et al. 2017) in which can be incorporated M^{n+} cations.

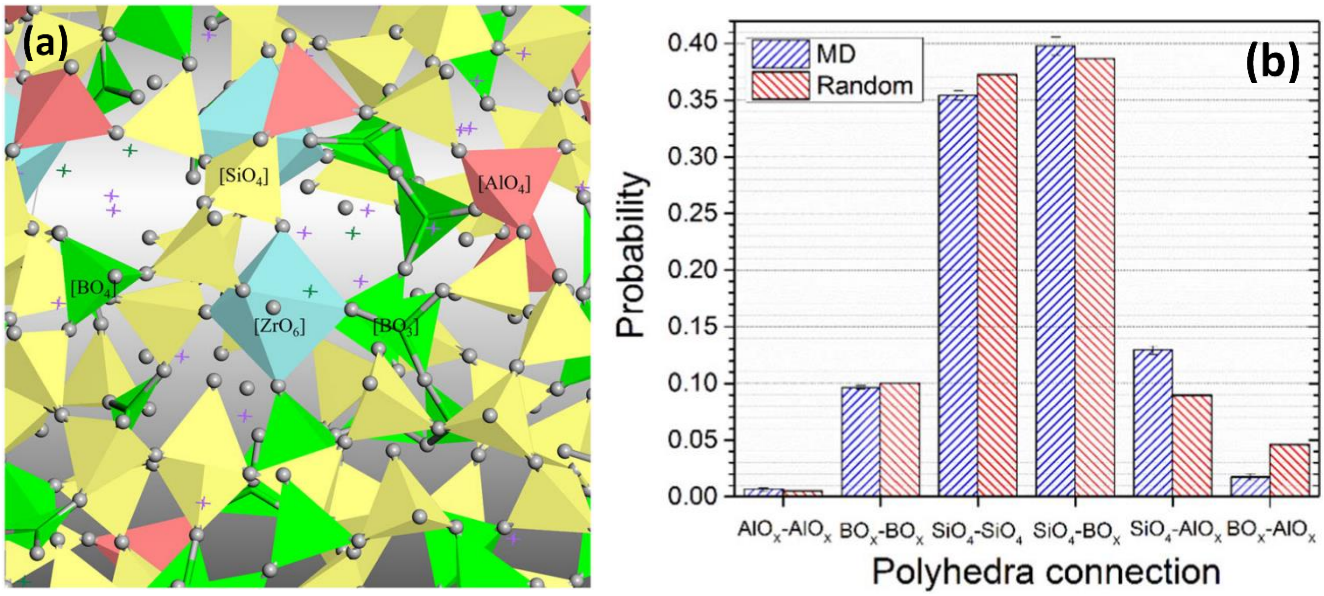

Figure 10. (a) Snapshot of a 6-oxides borosilicate glass structure with composition close to that of the ISG glass from molecular dynamics simulations showing the interconnection between SiO_4 (yellow), BO_3 and BO_4 (green), AlO_4 (pink) and ZrO_6 (blue) polyhedra. The purple and green crosses represent respectively sodium and calcium cations. (Lu X., Deng L., Kerisit S. and Du J. (2018) Structural role of ZrO_2 and its impact on properties of boroaluminosilicate nuclear waste glasses. *npj Mater. Degrad.* **2**, 19. p. 4. Reproduced with permission from Springer Nature) **(b)** Occurrence probability of different connections between SiO_4, BO_x (x = 3 or 4) and AlO_x (x = 4 (98%) and x = 3 or 5 (2%)) polyhedra in a 4-oxides borosilicate glass (SiO_2-B_2O_3-Al_2O_3-Na_2O) derived from

the ISG glass by converting CaO to Na_2O and ZrO_2 to SiO_2 under the same mole percentage. Molecular dynamics simulation results (blue) are compared to theoretical values by assuming a random distribution of network former atoms (red): the similarity of the results shows that the network former atoms tend to be randomly distributed. (Ren M., Deng L., and Du J. (2017). Bulk, surface structures and properties of sodium borosilicate and boroaluminosilicate nuclear waste glasses from molecular dynamics simulations. *J. Non-Cryst. Solid*s **476**, 87-94. p. 93. Reproduced with permission from Elsevier)

In comparison with cationic species, anionic species such as halide (F^-, Cl^-, I^-) and sulfur (S^{2-}) that may be present in several kinds of HLW are hardly soluble in borosilicate glasses because of the difficulty to connect them efficiently to the borosilicate network and their high tendency to volatilize during melting (Gin S., Jollivet P., Tribet M., Peuget S. and Schuller S. 2017). The facility to dissolve M^{n+} cations in borosilicate glasses structure depends on both their size and charge. Generally, the higher their cationic field strength F_s, the higher their tendency to impose their local environment with strong M-O bonds with the oxygen anions available in the glass structure and the lower their solubility due to an increasing phase separation or crystallization tendency (the field strength of a cation in an oxide can be defined as $F_s = Z/d^2$ where Z is the cation charge and d is the mean cation-oxygen distance). When M^{n+} cations are linked to the borosilicate network, they form MO_n polyhedra with BOs or/and NBOs and their preference to connect to NBOs increases with F_s. For instance, lanthanide Ln^{3+} cations are preferentially connected to NBOs whereas alkali cations have both NBOs and BOs in their coordination sphere (Du J. and Cormack A. N. 2005). The lowest F_s cations such as alkalis and alkaline-earths insure local charge compensation around MO_n polyhedra and complete the bond valence of the oxygen atoms engaged in M-O-Si bonds (see the example of NdO_n polyhedra charge compensated by Na^+ and Ca^{2+} cations in Fig. 1), these cations are thus essential to facilitate the dissolution of M^{n+} cations in the glassy network (formation of NBOs + charge compensation of MO_n polyhedra), and they strongly contribute to its structural flexibility. Nevertheless, peraluminous borosilicate glass compositions defined by an excess of Al^{3+} cations in comparison with the amount of alkali and alkaline-earth cations have also been envisaged as potential wasteforms with enhanced physical and chemical properties in comparison with peralkaline borosilicate glasses because of the possibility of high F_s elements present in HLW such as lanthanides to act as charge compensators of AlO_4^- units (Gasnier E., Bardez-Giboire I., Montouillout V., Pellerin N., Allix M. et al. 2014, Piovesan V., Bardez-Giboire I., Fournier M., Frugier P., Jollivet P. et al. 2018).

Let us now consider successively the incorporation in the structure of nuclear borosilicate glasses of several families of elements present in HLW.

Incorporation of alkalis and alkaline-earths

The alkali and alkaline-earth cations that may be present in HLW (Cs^+, Rb^+, Mg^{2+}, Ba^{2+}, Sr^{2+}) play the same role of modifier or charge compensator as the alkali and alkaline-earth cations brought by the glass frit, they are thus generally easily dissolved in glass structure. Nevertheless, depending on waste composition, they may partly separate and crystallize with anionic entities poorly soluble in the melt and in the glass such as orthophosphate (PO_4^{3-}) and molybdate (MoO_4^{2-}) polyanions (Fig. 3), also coming from the waste but that are not connected to the borosilicate network (the alkali and alkaline-earth cations Na^+, Li^+ and Ca^{2+} brought by the glass frit may also separate with these anionic entities). Such separation can be a problem if for instance the long-lived ^{135}Cs isotope crystallizes in poorly durable phases such as alkali molybdates because Cs^+ has a high mobility in geological environment. Nevertheless, the crystallization of such alkali-rich phases may also lead to an increase of the overall wasteform durability if they do not percolate trough the surrounding glass (see below, the case of molybdenum) (Nicoleau E., Schuller S., Angeli F., Charpentier T., Jollivet P. et al. 2015).

Incorporation of transition metals

Numerous transition metals are present in HLW, originating either from nuclear fuel fission (Tc, Mo, Zr…), from reprocessing equipments (Fe, Ni, Cr) or from metallic cladding (Zr). Some of these metals can be particularly problematic during vitrification process or for the long-term properties of the wasteforms because they can be highly volatile as Tc (for which all isotopes are radioactive) or may exhibit low solubility in the melt and during cooling because of their high tendency to phase separate (Mo) and/or to crystallize (Cr) which limits the waste loading, if one seek to obtain wasteforms without crystals.

The case of technetium

As Tc^{7+} is very volatile during melting (it is present as very mobile TcO_4^- anions not connected to the borosilicate network), it is important to try to increase its retention by operating under more reducing conditions in order to promote Tc^{4+} that is less volatile, probably because it is present as less mobile TcO_6 octahedral units connected to the borosilicate network (Muller I. S., McKeown D. A. and Pegg I. L. 2014). About 0.4 wt% TcO_2 is present in the R7T7 glass. In laboratory scale experiments, rhenium that belongs to the same column of the periodic table as Tc, is frequently used as a non-radioactive surrogate for Tc (Goel A., McCloy J. S., Windisch C. F., Riley B. J., Schweiger M. J. et al. 2013).

The case of chromium

Chromium is poorly soluble in borosilicate melts and the R7T7 glass contains about 0.5 wt% Cr_2O_3. It is non-radioactive and only comes from the reprocessing process (tank and metallic melter corrosion). It is mainly present as Cr^{3+} (mixed with Cr^{6+} whose proportion depends on the redox melting conditions) in borosilicate glasses with a strong stabilization in octahedral CrO_6 environment. This may explain the high crystallization tendency of Cr_2O_3 or spinel phases such as $ZnCr_2O_4$ in the presence of spinel-forming components such as ZnO (Fig. 8) which may lead to deleterious effects on melters performance (Hrma P., Vienna J. D., Wilson B. K., Plaisted T. J. and Heald S. M. 2006).

The case of zirconium

Zirconium is both a fission product (with about 20% ^{93}Zr, a long-lived isotope with half-life of 1.5 million years) and an additional element coming from the fuel metallic cladding (zircalloy). It can also be present in the glass frit added to the waste to improve glass durability. The R7T7 glass contains about 2.7 wt% ZrO_2. Zirconium only occurs as Zr^{4+} in borosilicate glasses and is preferentially located in octahedral ZrO_6 sites connected to the silicate network by strong Zr-O-Si bonds, but Zr-O-B may also exist (Galoisy L., Pélegrin E., Arrio M-A., Ildefonse P., Calas G. et al. 1999, Lu X., Deng L., Kerisit S. and Du J. 2018) (Fig. 10). Alkali and alkaline-earth cations insure local electroneutrality and complete the bond valences of oxygen atoms surrounding zirconium that thus acts as a reticulating agent because it induces a decrease of the NBOs proportion. As consequence, the addition of ZrO_2 to the glass leads to significant increase of T_g. Moreover, ZrO_6 units would be preferentially charge compensated rather than the BO_4 units (Angeli F., Charpentier T., Gaillard M. and Jollivet P. 2008). Consequently, in spite of its high F_s, Zr^{4+} is usually rather well incorporated in the network of nuclear borosilicate glasses if there is enough charge compensators available. Nevertheless, the crystallization of Zr-rich phases such as ZrO_2 and $ZrSiO_4$ can occur for particular borosilicate glass compositions, but these phases are well-known for their high chemical durability (Chen H., Marcial J., Ahmadzadeh M., Patil D. and McCloy J. 2020). Moreover, it has been shown that ZrO_2 addition to borosilicate glasses induced a decrease of the initial dissolution rate in water but lead to a greater degree of alteration for longer times (Cailleteau C., Angeli F., Devreux F., Gin S., Jestin J. et al. 2008) which can be explained by the local strengthening of glass network in Zr neighborhood due to the strong Zr-O-Si bonds. Finally all zirconium remains in the alteration layer on glass surface (Angeli F., Charpentier T., Gaillard M. and Jollivet P. 2008).

The case of molybdenum

Molybdenum is a rather abundant stable fission product present in HLW solutions (Fig. 3) that mainly occurs as Mo^{6+} in nuclear borosilicate glasses prepared in oxidizing conditions. Due to its high F_s, Mo^{6+} occurs as isolated and mobile molybdate (MoO_4^{2-}) tetrahedral entities in the depolymerized regions of the structure rich in alkali and alkaline-earth cations (Fig. 11). Indeed, Mo-O-Si bonds between Mo and the glassy network cannot exist according to bond valence considerations because in such a situation the oxygen atom connecting Mo and Si would be overbonded (Calas G., Legrand M., Galoisy L. and Ghaleb D. 2003).

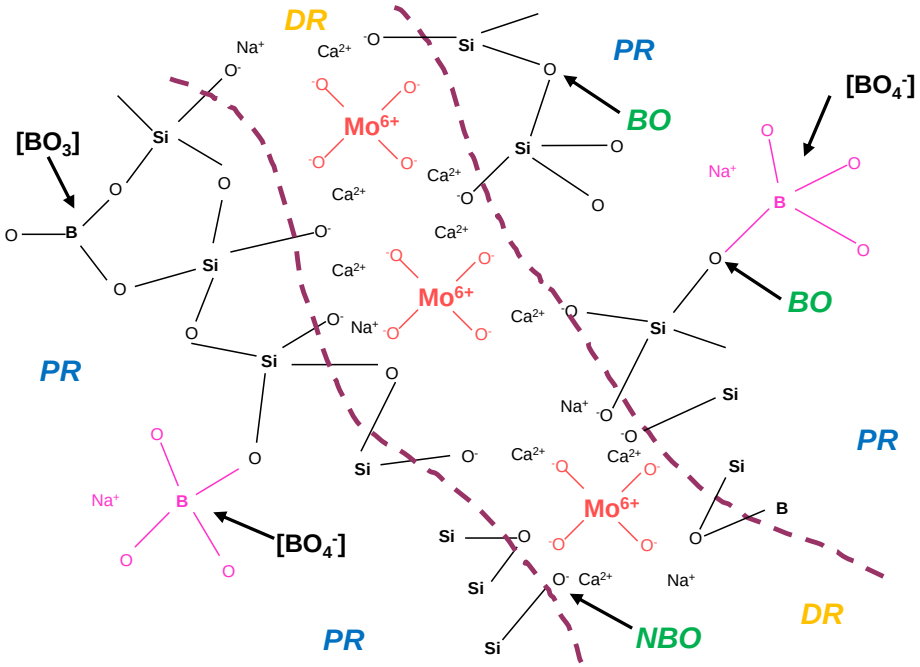

Figure 11. Structural scheme showing the way molybdenum may enter in borosilicate nuclear glasses as isolated MoO_4^{2-} entities located in the depolymerized regions (DR) of the glassy network rich in non-bridging oxygen atoms (NBOs) and alkali + alkaline-earth cations (here Na^+ and Ca^{2+}). Polymerized regions (PR) rich in bridging oxygen atoms (BOs) are also shown.

Similarly to other highly charged (+5, +6, +7) elements present as isolated oxoanionic species in borosilicate glasses (PO_4^{3-}, CrO_4^{2-}, TcO_4^-), Mo is thus poorly soluble in the structure of borosilicate glasses (solubility ~ 1-3 mol% MoO_3) and has a high tendency to phase separate during melting and cooling, and then to crystallize as alkali and alkaline-earth molybdates (Fig. 12). For instance, during vitrification process, the presence of important amounts of molybdenum in waste can lead to the formation of a Mo-rich phase called “yellow phase” that separates from the glass melt during vitrification and is undesirable both for melter operations and wasteform properties which limits waste loading (McKeown D. A, Gan H. and Pegg I. L.

2017). The situation is different for phosphate glasses where Mo^{6+} can be connected to the phosphate network trough Mo-O-P bonds with a high fraction of MoO_6 entities, which explains the higher MoO_3 solubility in this kind of glass (Santagneli S. H., de Araujo C. C., Strojek W., Eckert H., Poirier G. et al. 2007). For instance, up to 83 mol% MoO_3 can be dissolved in pure P_2O_5 glass (Bridge B. and Patel N. D. 1986).

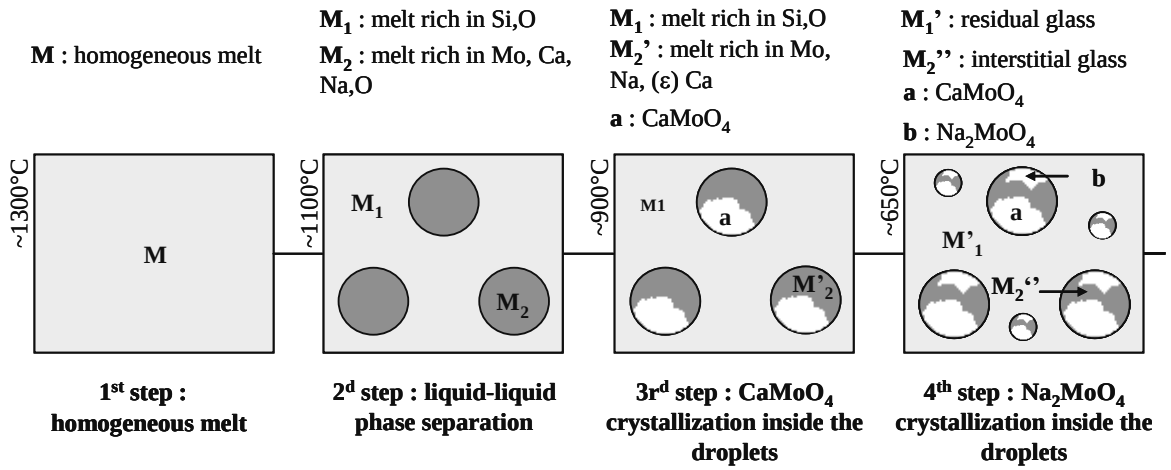

Figure 12. Scheme showing the microstructural evolution during melt cooling of a Mo-rich soda-lime borosilicate glass showing 4 steps: (1) homogeneous melt M during melting (T > 1100°C), (2) liquid-liquid phase separation (M_1 +M_2) during cooling forming droplets M_2, (3) $CaMoO_4$ crystallization (T ≤ 900°C) and (4) Na_2MoO_4 crystallization (T ≤ 650°C) in the droplets M_2 (Based on Magnin M. (2009) Study of phase separation and crystallization phenomena in soda-lime borosilicate glass enriched in MoO_3 (in French). PhD of the University Pierre and Marie Curie. Paris, France. p. 136. https://inis.iaea.org/collection/NCLCollectionStore/_Public/42/039/42039802.pdf)

As alkaline-earth molybdates such as $CaMoO_4$ (powellite) are much less soluble in water than alkali molybdates that may also incorporate radioactive Cs, if crystallization cannot be avoided - as in Mo-rich waste (Fig. 4) - it is strongly preferable to orientate crystallization towards alkaline-earth molybdates. This can be performed for instance by increasing the B_2O_3 content in Mo-rich borosilicate glasses. As BO_4^- units are preferentially charge compensated by alkali, their presence in the glassy network (Fig. 1) induces an increase of the proportion of alkaline-earth cations in the surrounding of MoO_4^- entities which promotes the crystallization of alkaline-earth molybdates and the expense of alkali molybdates (Caurant D., Majérus O., Fadel E., Lenoir M., Gervais C. et al. 2007, Magnin M., Schuller S., Mercier C., Trébosc J., Caurant D. et al. 2011) (Figs. 12 and 13).

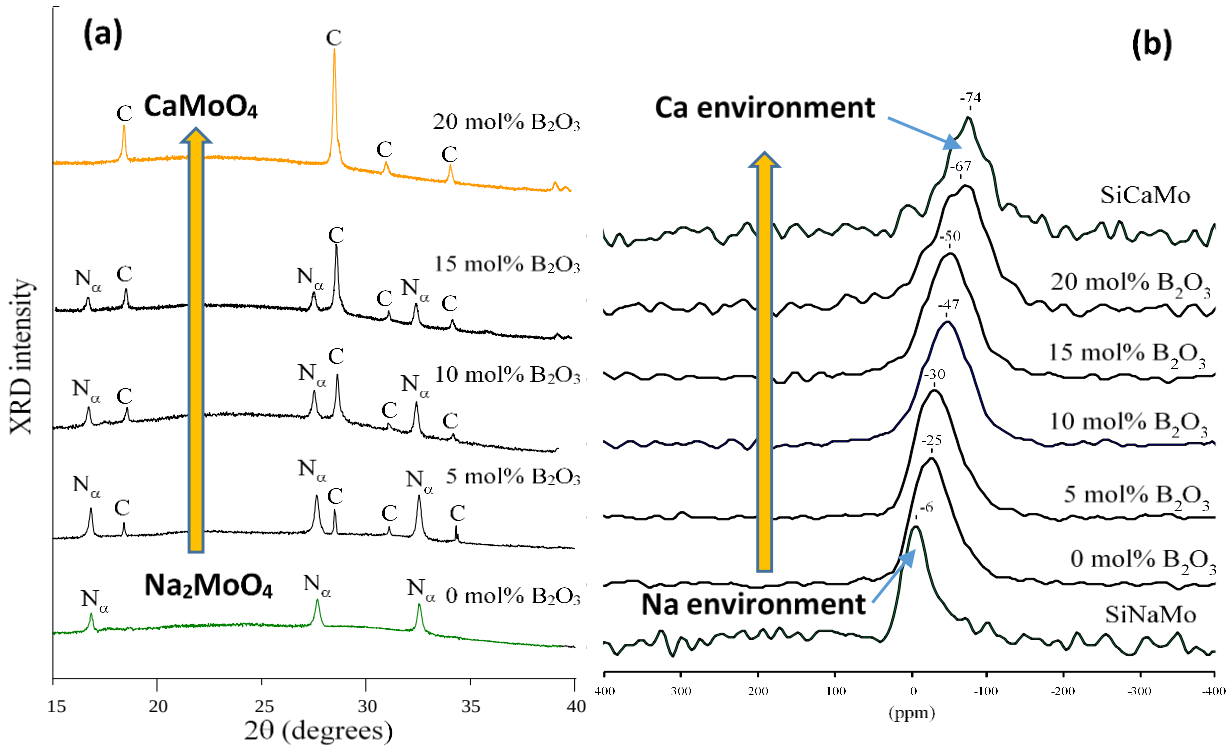

Figure 13. (a) XRD patterns evolution with B_2O_3 content of slowly cooled soda-lime borosilicate glasses bearing about 2.5 mol% MoO_3 showing the increasing $CaMoO_4$ (C) crystallization tendency at the expense of Na_2MoO_4 (N_α) when the B_2O_3 content increases. (b) Evolution with B_2O_3 content of ^{95}Mo MAS NMR spectra of quenched soda-lime borosilicate glasses bearing about 2.5 mol% MoO_3 compared with spectra of reference glasses of the SiO_2-CaO-MoO_3 (SiCaMo) and SiO_2-Na_2O-MoO_3 (SiNaMo) systems showing the progressive Ca-enrichment in the environment of MoO_4^{2-} entities when the B_2O_3 content increases. (Modified from (Magnin M., Schuller S., Mercier C., Trébosc J., Caurant D., Majérus O., Angéli F. and Charpentier C. (2011) Modification of molybdenum structural environment in borosilicate glasses with increasing content of boron and calcium oxide by ^{95}Mo MAS NMR. *J. Am. Ceram. Soc.* **94**, 4274-4282. p. 4277 and 4278). Permission from John Wiley and Sons)

The presence in HLW or the addition to the melt of certain elements such as lanthanides and vanadium can help the incorporation of molybdenum in borosilicate melts and glasses. For instance, it has been shown that the progressive addition of Nd_2O_3 to a Mo-rich borosilicate glass enables to suppress molybdate crystallization during melt cooling (Chouard N, Caurant D., Majérus O., Dussossoy J. L., Ledieu A. et al. 2011). This beneficial effect of lanthanides on molybdenum solubility has also been put in evidence for other lanthanides of various sizes (La, Ce, Sm, Er, Yb) (Patil D. S., Konale M., Gabel M., Neill O. K., Crum J. V. et al. 2018). Two alternative structural models have been proposed to explain this effect of lanthanides, all considering that Ln^{3+} and MoO_4^{2-} ions are located in the same regions of the glass structure (Chouard N, Caurant D., Majérus O., Dussossoy J. L., Ledieu A. et al. 2011, Brehault A., Patil D., Kamat H., Youngman R. E., Thirion L. M. et al. 2018). As lanthanides are already present

in significant concentration in HLW (Fig. 3), their presence may participate to molybdenum stabilization in nuclear borosilicate glasses. It has also been reported that the addition of vanadium as V_2O_5 in Mo-rich borosilicate glasses would help to stabilize MoO_4^{2-} and to avoid yellow phase formation, the presence of VO_4^{3-} tetrahedral units sharing alkali cations with MoO_4^{2-} would be responsible for this effect (McKeown D. A, Gan H. and Pegg I. L. 2017). Recent studies also indicate that the addition of P_2O_5 to Mo-rich borosilicate glasses would help MoO_3 dissolution in the melt, probably by forming phosphorus-rich regions able to incorporate molybdenum (Prakash A. D., Singh M., Mishra R. K., Valsala T. P., Tyagi A. K. et al. 2019, Krishnamurthy A., Nguyen T., Fayek M., Shabaga B. and Kroeker S. 2020). Magnesium aluminosilicate glass compositions have also been reported to incorporate more molybdenum than borosilicate glasses (Tan S., Ojovan M. I., Hyatt N. C. and Hand R. J. 2015). It is interesting to indicate that in spite of their low durability the separation or/and crystallization of alkali molybdates in borosilicate glasses does not necessarily imply a decrease of the chemical durability in water of the overall wasteform. For example, the separation of isolated (i.e. non-percolating) sodium molybdates particles in a borosilicate glass may lead to an increase of the surrounding glass durability (due to Na_2O depletion and decrease of NBOs proportion) which controls the alteration of the poorly durable sodium molybdate particles dispersed in the glass (Fig. 14) (Nicoleau E., Schuller S., Angeli F., Charpentier T., Jollivet P. et al. 2015).

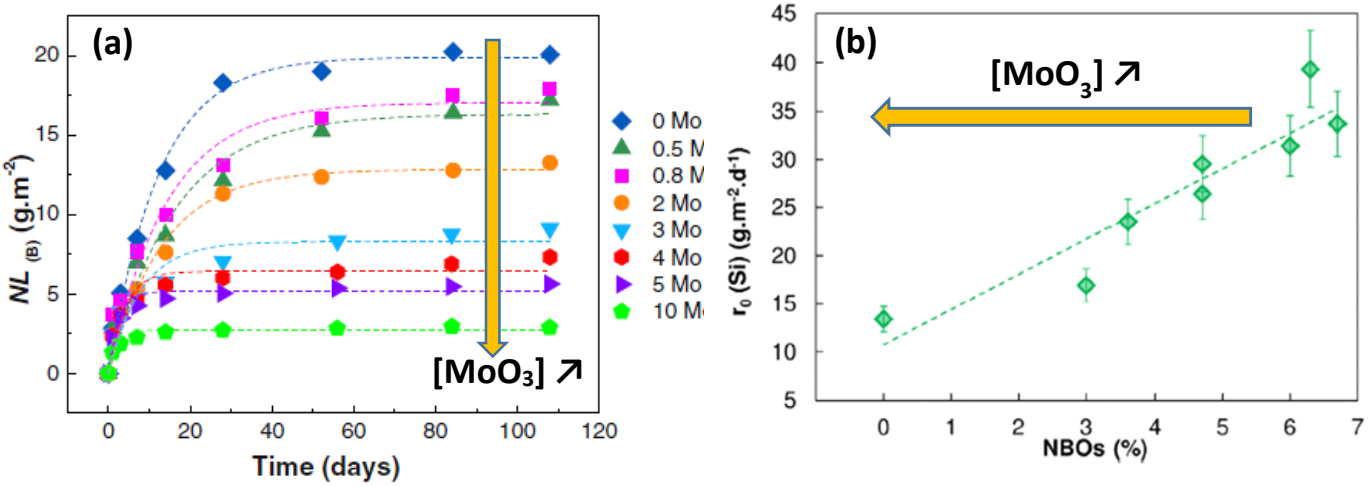

Figure 14. (a) Evolution with time of the normalized mass loss for boron during alteration at 90°C in water of a sodium borosilicate glass with increasing MoO_3 contents (0-10 mol%) showing an important decrease of the amount of glass altered. Above 1.4 mol% MoO_3 glasses where heterogeneous (phase separation + Na_2MoO_4 crystallization). (b) Evolution of the initial dissolution rate r_0 for Si for the same glass series as a function of the percentage of NBOs (that decreases with MoO_3 content). A clear correlation is observed between the decrease of r_0 of the glassy phase (where Si is located) and the drop in the number of NBOs (increase of the polymerization of

the glassy network). (Modified from Nicoleau E., Schuller S., Angeli F., Charpentier T., Jollivet P., Le Gac A., Fournier M., Mesbah A. and Vasconcelos F. (2015) Phase separation and crystallization effects on the structure and durability of molybdenum borosilicate glass. *J. Non-Cryst. Solids* **427**, 120-133. p. 130. Permission from Elsevier).

Incorporation of lanthanides and actinides

Lanthanides (Ln) with yttrium represent one of the most abundant family of FP in HLW (Fig. 3) where the four biggest Ln (La, Ce, Pr, Nd) represent more than 90 wt% of all Ln. Only a small fraction of lanthanides is radioactive (the longest-lived Ln isotope is ^{151}Sm with half-life of 93 years and low concentration) and all Ln are poorly soluble in water. Due to their $4f^n$ electronic configuration with deep 4f level, lanthanides mainly occur at oxidation state +III, except Ce that frequently exists as Ce^{3+} and Ce^{4+} depending on redox conditions. In comparison, the amount of actinides (An) in HLW is much weaker than that of lanthanides (Fig. 3) but they are all radioactive (α-radionuclides). They mainly consist in minor actinides (Np, Am, Cm) and small amounts of U and Pu. Because of their $5f^n$ electronic configuration, U, Np and Pu may occur at higher oxidation state than +III, but as the energy and the spatial extension of the 5f orbital drops rapidly with increasing actinides atomic number, heavier actinides (Am, Cm) behave more as lanthanides and only exist as Am^{3+} and Cm^{3+} in glasses (Eller, P. G., Jarvinen J. D., Purson J. D., Penneman R. A., Ryan R. R. et al. 1985). This is the reason why Ln^{3+} (such as Nd^{3+}) with close ionic radius to Am^{3+} and Cm^{3+} are frequently used as Am and Cm non-radioactive surrogates in laboratory experiments on nuclear glasses. It has also been shown that in borosilicate glasses Nd^{3+} and Am^{3+} behave similarly during crystallization (Bardez-Giboire I., Kidari A., Magnin M., Dussossoy J-L., Peuget S. et al. 2017)

The case of lanthanides

Despite their high F_s Ln^{3+} cations are usually well dissolved in nuclear borosilicate glasses. Nevertheless, for high waste loading the crystallization of Ln-rich phases may be observed during melt cooling such as $Ca_2Ln_8(SiO_4)_6O_2$ (apatite) (Fig. 7), and Ln borates and borosilicates depending on glass composition (Quintas A., Caurant D., Majérus O., Dussossoy J-L. and Charpentier T. 2008, Chen H., Marcial J., Ahmadzadeh M., Patil D. and McCloy J. 2020). Moreover, the size of Ln^{3+} cations may strongly impact the nature of RE-rich crystals and glass crystallization tendency (Loiseau P., Caurant D., Baffier N., Mazerolles L. and Fillet C. 2004, Quintas A., Caurant D., Majérus O., Dussossoy J-L. and Charpentier T. 2008, Kidari A., Dussossoy J-L., Brackx E., Caurant D., Magnin M. et al. 2012, Chen H., Marcial J., Ahmadzadeh M., Patil D. and McCloy J. 2020). Even if a phase like $Ca_2Ln_8(SiO_4)_6O_2$ exhibits

a good chemical durability, it tends to become amorphous and swell under self-irradiation due the α-decay of MA that can partly substitute for Ln in crystals structure (Weber W. J. 1983). This could then induce local strains and cracks in the surrounding glass (Weber W. J., Turcotte R.-P., Bunnel L. R., Roberts F. P. and Westsik J. H. 1979) depending on crystals size which would be problematic for the long-term behavior of wasteforms and requires to control their crystallization and particularly their size or to avoid Ln-rich phases formation, acting for instance on glass composition to improve Ln^{3+} solubility (Chouard N., Caurant D., Majérus O., Dussossoy J.-L., Loiseau P. et al. 2019). Moreover, it has been reported that the crystallization of $Ca_2Ln_8(SiO_4)_6O_2$ in borosilicate glasses tends to make them less durable against water alteration because of the evolution of both the composition (CaO and Ln_2O_3 depletion), the structure and the durability of the surrounding glass in comparison with homogeneous glass (Nicoleau E., Angeli F., Schuller S., Charpentier T., Jollivet P. et al. 2016). Nevertheless, glass-ceramics containing $Ca_2Ln_8(SiO_4)_6O_2$ or $NaLn_9(SiO_4)_6O_2$ crystals have been proposed as wasteform for actinides immobilization because of the capacity of apatite crystals to incorporate trivalent actinides in their structure (Caurant D., Majérus O., Loiseau P., Bardez I., Baffier N. et al. 2006, Zhao D., Li L., Davis L. L., Weber W. J. and Ewing R.C. 2000).

Whereas Ln_2O_3 is very weakly soluble in pure silica glass (strong phase separation tendency) due to the high F_s of Ln^{3+} ions that do not succeed to satisfy their environment because of the insufficient quantity of NBOs, and thus rapidly tend to form clusters, the addition of alkali and alkaline-earth oxides enables to strongly increase its solubility both by creating numerous NBOs and by bringing alkali and alkaline-earth cations that may ensure local charge compensation in the surrounding of LnO_n polyhedra as shown in Fig. 1. When added to silicate or borosilicate glasses, Ln_2O_3 usually act as modifier oxide forming NBOs (Fig. 15) and Ln^{3+} are linked to NBOs forming strong Ln-O-Si bonds which explains the raise of T_g with Ln_2O_3 content (Schaller T., Stebbins J. F. and Wilding M. C. 1999, Kidari A., Dussossoy J-L., Brackx E., Caurant D., Magnin M. et al. 2012, Gaddam A., Fernandes H. R., Tulyaganov D. U., Ferreira J. M. F. 2019). Moreover, the impact of La_2O_3 content on the alteration kinetics of borosilicate glasses showed that lanthanum improves their chemical durability in water and La^{3+} ions (as other Ln) are almost integrally retained in the alteration layer on glass surface (Molières E., Angeli F., Jollivet P., Gin S., Charpentier T. et al. 2013, Ménard O., Advocat T., Ambrosi J. P. and Michard A. 1998).

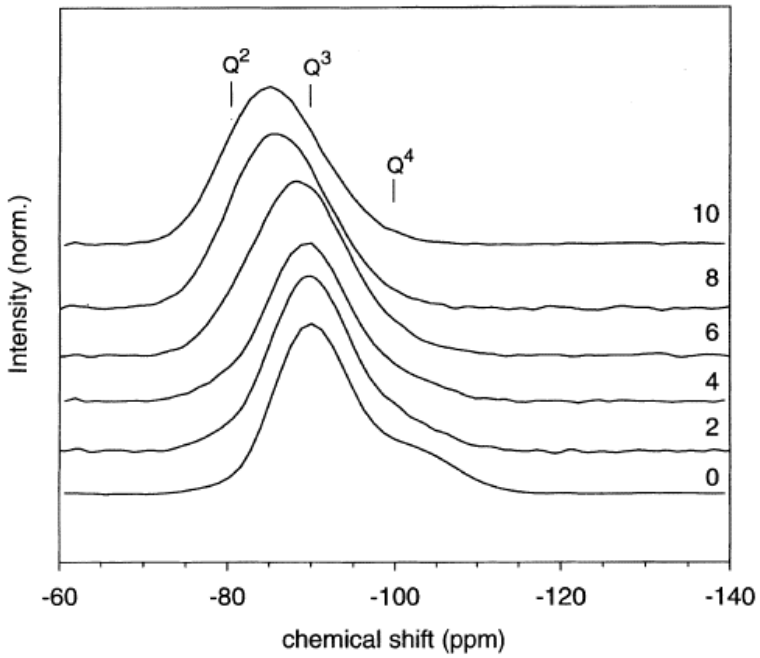

Figure 15. Evolution of ^{29}Si MAS NMR spectra when increasing La_2O_3 amounts (0-10 mol%) are added to the $75SiO_2$-$25Na_2O$ glass putting in evidence the depolymerization of the silicate network and the modifier role of La_2O_3 (Q^n represents SiO_4 tetrahedral units with n BOs). (Schaller T., Stebbins J. F. and Wilding M. C. (1999) Cation clustering and formation of free oxide ions in sodium and potassium lanthanum silicate glasses: nuclear magnetic resonance and Raman spectroscopic findings. *J. Non-Cryst. Solids* **243**, 146-157. p. 150. Reproduced with permission from Elsevier)

To be stabilized and uniformly dispersed in glass structure, Ln^{3+} needs to satisfy easily its environment finding enough alkali or alkaline-earth cations and NBOs (Angeli F., Charpentier T., Molières E., Soleilhavoup A., Jollivet P. et al. 2013). When adding increasing Ln_2O_3 amounts to glass, Ln^{3+} remains solubilized in glass network as long as there is enough charge compensators, but beyond this limit concentration the separation or crystallization of a Ln-rich phase can be observed (Fig. 16).

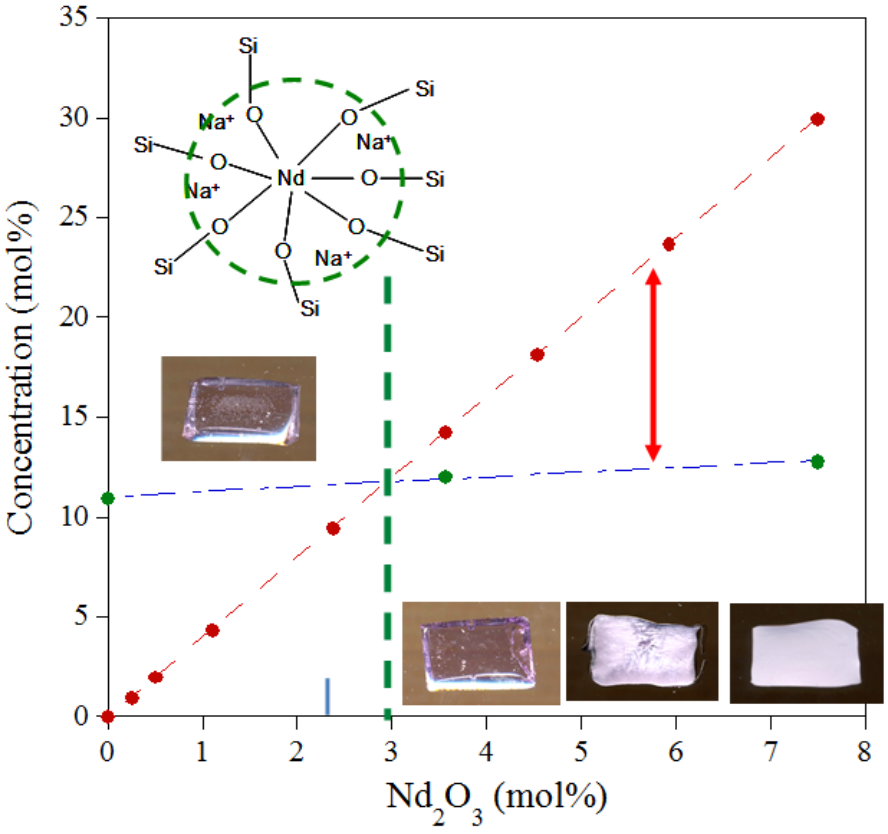

Figure 16. Evolution with the Nd_2O_3 content in a borosilicate glass ($64SiO_2$-$9.3B_2O_3$-$3.2Al_2O_3$-$15Na_2O$-$6.5CaO$-$2ZrO_2$ mol%): (in red) of the amount of Na_2O + CaO needed to compensate the negative charge excess of NdO_7 polyhedra (see Fig. 1) in glass structure (4 moles (Na_2O + CaO) for 1 mole Nd_2O_3); (in green) of the amount of Na_2O + CaO available both to charge compensate NdO_7 polyhedra and to supply NBOs for their formation, taking into account the amount of charge compensators used for the compensation of AlO_4^- and BO_4^- units deduced from NMR results. Above about 3 mol% Nd_2O_3 (vertical dotted green line) there is not enough NBOs and charge compensators available to enable the incorporation of Nd^{3+} as isolated NdO_7 entities which thus rapidly tend to agglomerate and to separate or crystallize as $Ca_2Nd_8(SiO_4)_6O_2$ phase (apatite) when the charge compensators deficiency increases (red arrow). The pictures of slowly cooled samples (6°C.min^{-1}) from the melt with increasing Nd_2O_3 content show their strong crystallization tendency when the amount of Na_2O + CaO becomes insufficient.

Al_2O_3 content also has an important effect on the stabilization of Ln^{3+} in borosilicate glasses. For instance, the addition of increasing Al_2O_3 amounts to a peralkaline borosilicate glass progressively destabilizes Ln^{3+} because aluminum (mainly present as AlO_4^- units) is charge compensated in priority compared to LnO_n polyhedra which induces a progressive depletion of charge compensators available for lanthanides, and the separation or crystallization tendency of Ln-rich phases increases. However, when the composition becomes peraluminous (i.e. when there is not enough alkali and alkaline-earth cations to compensate all AlO_4^- units), the solubility of Ln_2O_3 begins to increase because an increasing number of Nd^{3+} act as charge compensators of the excess AlO_4^- units (Fig 17), increasing their dispersion and thus their

solubility in glass structure. Such peraluminous borosilicate glasses have been envisaged to immobilize waste with high Ln_2O_3 contents because of their ability to incorporate higher Ln_2O_3 quantities than peralkaline glasses and they exhibit higher chemical durability (Gasnier E., Bardez-Giboire I., Montouillout V., Pellerin N., Allix M. et al. 2014, Piovesan V., Bardez-Giboire I., Fournier M., Frugier P., Jollivet P. et al. 2018).

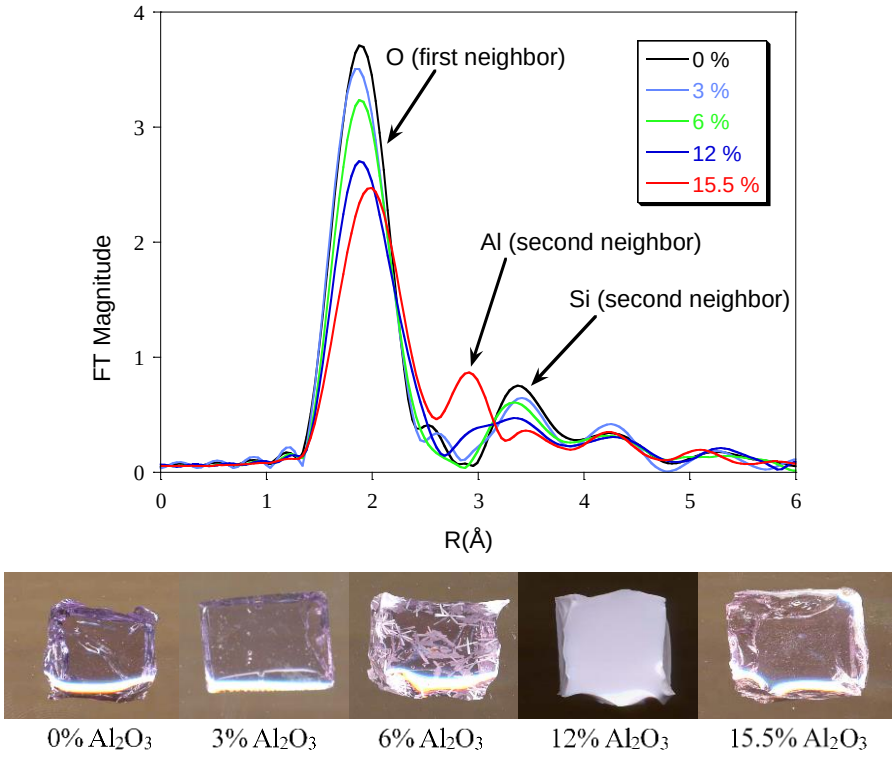

Figure 17. Evolution of the Fourier transforms of the Nd L_{III}-edge EXAFS spectra of neodymium in a borosilicate glass ($61.8SiO_2$-$9B_2O_3$-$16.5Na_2O$-$7.2CaO$-$2ZrO_2$-$3.5Nd_2O_3$ mol%) to which increasing Al_2O_3 amounts (0-15.5 mol%) were progressively substituted for Na_2O + CaO, keeping constant all other concentrations. All compositions were peralkaline except the one with 15.5 mol% Al_2O_3 that was peraluminous and for which the presence of Al as second neighbor of Nd is put in evidence (Nd^{3+} acts as charge compensator of AlO_4^- units inducing a decrease of the second neighbor distance). The pictures given at the bottom of the curves show the evolution of the aspect of glasses after cooling from the melt at 6°C.min^{-1}. No crystals were observed with 0 and 3 mol% Al_2O_3, but crystals ($Ca_2Nd_8(SiO_4)_6O_2$) and phase separation (100 nm Nd-rich droplets) were detected respectively with 6 and 12 mol% Al_2O_3 because of the decreasing amount of Na_2O + CaO available to enable Nd^{3+} ions solubilization. However, when the glass became peraluminous (15.5 mol% Al_2O_3), Nd^{3+} ions were again dispersed in glass structure. (Based on Bardez I. (2004) Study of the structural characteristics and properties of glasses rich in rare earths intended for the immobilization of fission products and long-lived elements (in French). PhD of the University Pierre and Marie Curie. Paris, France. https://pastel.archives-ouvertes.fr/pastel-00001075. p. 178.)

The case of actinides

While the chemical properties and the behavior of Am and Cm in borosilicate glasses appear close to that of trivalent lanthanides such as Nd (oxidation state +III, similar size, deep 4f and 5f levels) that can be used as Am or Cm surrogates, this is not the case for lighter actinides U, Np and Pu. Indeed, these three actinides may exit in different oxidation states (U^{4+}, U^{5+}, U^{6+}, Np^{3+}, Np^{4+}, Np^{5+}, Pu^{3+}, Pu^{4+}) depending on the conditions of glass preparation (temperature and redox). Plutonium mainly occurs as Pu^{4+} ions in nuclear glasses prepared under neutral or oxidizing conditions and it is only under strongly reducing conditions that almost all Pu^{4+} ions can be reduced to Pu^{3+} ions (Cachia J.-N., Deschanels X., Den Auwer C., Pinet O., Phalippou J. et al. 2006, Deschanels X., Peuget S., Cachia J. N. and Charpentier T. 2007). Neptunium exits as Np^{3+} only in glasses melted under strongly reducing conditions and mainly as Np^{4+} + Np^{5+} in glasses melted under more oxidizing conditions, whereas uranium is present as U^{4+} in glasses melted under reducing conditions and as both U^{5+} and U^{6+} if glasses are melted in oxidizing conditions (Gin S., Jollivet P., Tribet M., Peuget S. and Schuller S. 2017). Because of their lower F_s, trivalent actinides (Pu^{3+}, Am^{3+}, Cm^{3+}) are generally more soluble in glasses that actinides with higher oxidation states. This is true for plutonium whose solubility of Pu^{3+} is significantly higher than that of Pu^{4+}. For instance, Pu solubility can be increased from 2.5 (melting in air without reducing agent) to more than 4 wt% PuO_2 (melting in Ar with reducing agent) in a borosilicate glass (Cachia J.-N., Deschanels X., Den Auwer C., Pinet O., Phalippou J. et al. 2006). However, in the case of the highest uranium and neptunium oxidation states (U^{6+}, Np^{5+}) the situation is different because these elements would occur respectively as highly covalent linear uranyl (UO_2^{2+}) and neptunyl (NpO_2^{+}) entities (Gin S., Jollivet P., Tribet M., Peuget S. and Schuller S. 2017). These entities would be more soluble than the lower oxidation states of U and Np because of their easy dissolution in the depolymerized regions of the borosilicate glass structure where there would be connected to the NBOs of the network and charge compensated by modifier cations as it has been proposed for uranyl entities (Fig. 18) (Connelly A. J., Hyatt N. C., Travis K. P., Handa R. J., Stennett M. C. et al. 2013). Structural studies performed on Pu^{3+} and Cm^{3+} in borosilicate glasses showed that these species are well dispersed in glass structure and are respectively located in 8- and 7-fold coordinated sites (Deschanels X., Peuget S., Cachia J. N. and Charpentier T. 2007). Concerning the immobilization of Pu-rich waste in glassy wasteforms, it has been shown that lanthanide borosilicate glasses containing more than 40 wt% Ln_2O_3 (La_2O_3, Nd_2O_3, Gd_2O_3) were able to incorporate up to about 10 wt% PuO_2 whereas borosilicate glasses may solubilize only up to about 2 wt% and are less durable (Shiryaev A. A., Zubabichus Y. V., Stefanovsky S. V.,

Ptashkin A. G. and Marra J.C. 2009). As lanthanides, due to their very weak solubility in water, Am, Cm and Pu are almost totally retained in the alteration layer on glass surface, while the retention of Np and U in this layer may be lower depending on their oxidation state in the aqueous medium (Gin S., Jollivet P., Tribet M., Peuget S. and Schuller S. 2017, Ménard O., Advocat T., Ambrosi J. P. and Michard A. 1998).

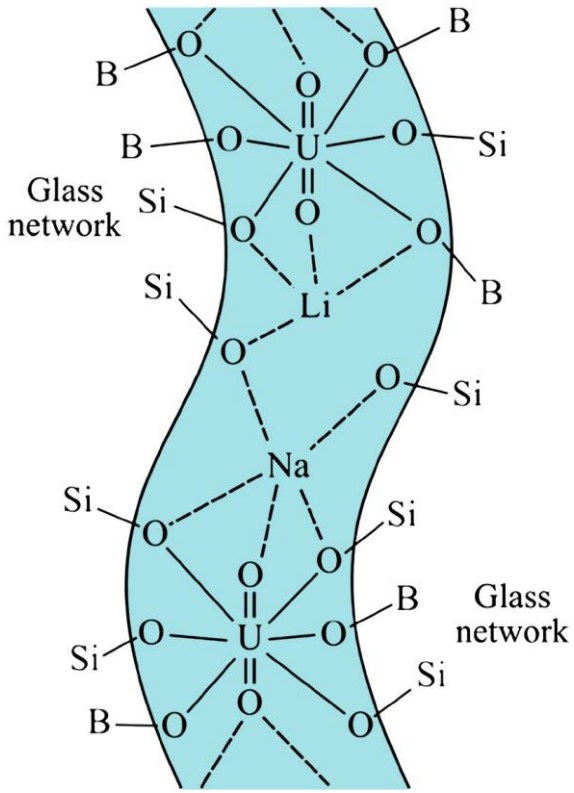

Figure 18. Structural scheme showing the way UO_2^{2+} (uranyl) entities could be incorporated in the depolymerized regions of a borosilicate glass. (Connelly A. J., Hyatt N. C., Travis K. P., Handa R. J., Stennett M. C., Gandya A. S., Brownb A. P. and Apperley D. C. (2013) The effect of uranium oxide additions on the structure of alkali borosilicate glasses. *J. Non-Cryst. Solids* **378**, 282-289. p. 288. Reproduced with permission from Elsevier)

Long-term behavior of nuclear glasses

As it is usually considered that HLW must be isolated from the biosphere at least until their radiotoxicity level will drop back to the radiotoxicity level of the initial uranium ore used to prepare the fuel (Fig. 2), glassy wasteforms must keep their containment properties for a very long time, at least several tens of thousands of years. For this, they must exhibit very good long-term behavior concerning both their resistance against the self-irradiation induced by the decay of the radionuclides incorporated in their structure and their resistance against alteration by water (liquid or vapor) that may be in contact with glass during geological disposal.

Self-irradiation resistance of nuclear glasses

The presence of high quantities of α and β radioactive elements (FP + MA) in nuclear glasses will induce numerous atomic displacements during their storage and disposal (Table 3). Indeed, during the α-decay of actinides, the α-recoil nuclei (with 80-120 keV energy) lose their energy in elastic collisions with the nuclei of their neighborhood and the α-particles produced (helium nuclei with 4-5 MeV energy) deposit their energy mainly by ionization processes but also by elastic collisions at the end of their paths. For each α-decay about 2400 atomic displacements are induced in glass structure by the emitted α-particle and the recoil of the new nucleus. For β-particles (electrons) and γ-radiation, the energy transfer is dominated by ionization and electronic excitation processes and the effects on glass structure are expected to be much weaker because of the very low number of atomic displacements. Nevertheless, due to the short half-live of abundant FP such ^{137}Cs and ^{90}Sr, β-decays are the main source of radioactivity and heat generation in the first 500 years, while after this period MA become the main source (Fig. 2).

Irradiation	**Number of events after 10^4 years**	**Range**	**Number of atomic displacements per event**
α-decay α-particle recoil nuclei	10^9	 ~ 20 µm 30 nm	 ~ 400 ~ 2000
β-decay	7.10^{19}	~ 1 mm	~ 1
γ	2.10^{19}	~ 2 cm	<< 1

Table 3. Characteristics of α, β and γ radiations in nuclear glasses due to fission products and minor actinides. (Gin, Jollivet, Tribet et al. 2017)

While in ceramics the accumulation of atomic displacements frequently leads to amorphization (destruction of the long-range order) and swelling (increase of the volume) (Weber W. J., Ewing R. C., Catlow C. R. A., de la Rubia T. D., Hobbs L. W. et al. 1998), the effect of self-irradiation on the structure and properties is expected to be weaker for nuclear glasses that are already amorphous. In order to evaluate the impact of irradiation damages on the structure and the physical and containment properties of nuclear glasses during storage and disposal, different kinds of accelerated tests are performed (Weber W. J. 2014). For instance, in order to simulate the effect of α-decays on glasses, samples can be prepared by incorporating short-lived actinides such as ^{238}Pu or ^{244}Cm (with half-lives of respectively 87 and 18 years) or external irradiation experiments with charged particles (heavy ions, α-particles) can be performed on inactive samples (Weber W. J., Ewing R. C., Angell C. A., Arnold G. W., Cormack A. N. et al. 1997). Molecular dynamics is also used to simulate the displacement cascades generated in borosilicate glasses by heavy nuclear projectiles which is very helpful to understand the

structural effects of α-decays (Peuget S., Delaye J.-M. and Jégou C. 2014). The effects of γ-irradiation can be simulated using radioactive external sources and β-irradiation can be simulated by external irradiation with electrons (Van de Graaff accelerator). Internal and external irradiation experiments simulating α-decays showed that for borosilicate glasses with composition close to that of the R7T7 nuclear glass, the density only slightly decreases (< 1%) (Fig. 19) and an improvement of mechanical properties is observed (~ 30% hardness reduction and increased resistance to cracking) (Peuget S., Cachia J.-N., Jégou C., Deschanels X., Roudil D. et al. 2006, Peuget S., Delaye J.-M. and Jégou C. 2014).

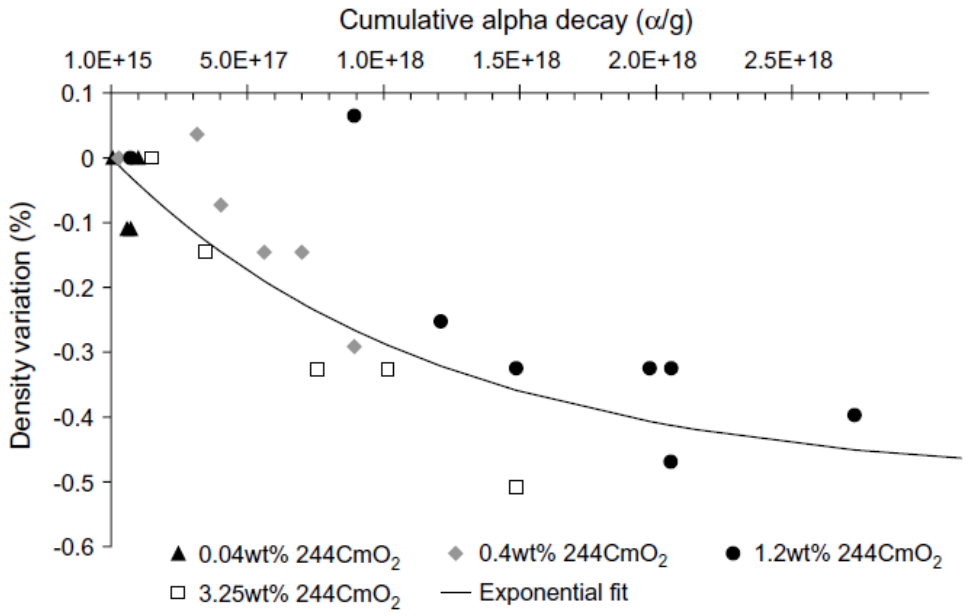

Figure 19. Evolution versus the α-decay cumulative dose of the density of a borosilicate glass doped with ^{244}Cm. A cumulative dose of about 3.10^{18} α/g corresponds to several thousand years of storage of active nuclear borosilicate glasses. (Peuget S., Cachia J.-N., Jégou C., Deschanels X., Roudil D., Broudic V., Delaye J.M. and Bart J.-M. Irradiation stability of R7T7-type borosilicate glass. *J. Nucl. Mater.* **354** (2006) 1-13. p. 7. Reproduced with permission from Elsevier)

The behavior in glass structure of helium atoms formed after α-decays and capture of 2 electrons by each α-particle and the consequences of their possible accumulation in glass structure remain to be clearly evaluated. However, the amount of helium generated in nuclear glasses used for commercial HLW immobilization would be only around 0.1-1 at% after 10^6 years and the formation of bubbles of significant size (> 10 nm) has not been observed at room temperature (Gin S., Jollivet P., Tribet M., Peuget S. and Schuller S. 2017, Peuget S., Delaye J.-M. and Jégou C. 2014). Studies have also been performed to evaluate the impact of α-decays on the chemical durability of glasses. Lixiviation tests have been carried out in water on

externally irradiated or short-lived actinides-doped borosilicate glasses. Whereas studies performed on self-irradiated and externally irradiated borosilicate nuclear glasses previously concluded that α-activity has no significant impact on the glass alteration rate by water (Peuget S., Broudic V., Jégou C., Frugier P., Roudil D. et al. 2007), more recent works show non-negligible impact of radiation damage on their alteration rate (Tribet M., Mir A.H., Gillet C., Jegou C., Mougnaud S et al. 2020), which may affect to some extent the containment properties during disposal on the very long-term. Moreover, the alteration rate in water tends to increase if irradiated glasses are previously altered by water in vapor phase, which is expected to occur for a long time during disposal before alteration with liquid water (Bates J. K., Seitz M. G. and Steinler M. J. 1984, Majérus O., Lehuédé P., Biron I., Alloteau F., Narayanasamy S. et al. 2020). The impact of transmutation of radioactive elements present in nuclear glasses is also important to consider. The transmutation of FP such as ^{137}Cs and ^{90}Sr are accompanied by important valence and ionic radius changes ($Cs^{+} \rightarrow Ba^{2+}$ and $Sr^{2+} \rightarrow Y^{3+} \rightarrow Zr^{4+}$) that can be easily accommodated in the flexible structure of nuclear glasses that contains high amounts of NBOs and charge compensators. For MA, as decay products are also actinides, they are expected to be incorporated similarly in glass structure (Gin S., Jollivet P., Tribet M., Peuget S. and Schuller S. 2017).

The effect of self-irradiation on the structure of the glassy network of borosilicate glasses has been examined by structural characterizations on irradiated samples. Concerning β-decays, external irradiation of borosilicate glasses by electrons showed the formation of paramagnetic defects (put in evidence by EPR, Electron Paramagnetic Resonance), the evolution of the polymerization of the glassy network and the formation of dissolved molecular oxygen (Malchukova E., Boizot B., Petite G. and Ghaleb D. 2009). However, the presence of transition metals such as chromium and iron may significantly diminish the amount of defects and the structural changes induced under β-irradiation. This effect can be attributed to the capacity of transition metals to change their state charge by electron trapping leading to stable valence states, but this would not suppress the defects produced by hole trapping (electron holes being generated in glasses during electron irradiation) (Malchukova E., Boizot B., Petite G. and Ghaleb D. 2009). Concerning α-decays, NMR investigations of ^{244}Cm doped ISG glass showed only small modifications of the local structure: a slight variation of the environment of AlO_4^- units and a weak decrease (~ 7%) of the proportion of BO_4^- units were observed (Fig. 20). The decrease of the proportion of BO_4^- units under α self-irradiation was explained by local melting + rapid quenching effects in glass structure due to α-recoils and α-particles (Charpentier T., Martel L., Mir A. H., Somers J., Jégou C. et al. 2016), similar to the well-known effect of the

quenching rate on the $BO_4^- \leftrightarrow BO_3$ equilibrium in borosilicate glasses (Angéli F., Charpentier T., Jollivet P., de Ligny D., Bergler M. et al. 2018). Moreover, during their displacement in glass structure, the energy loss of α-particles would partly repair the regions damaged by α-recoils as shown by sequential and simultaneous ion irradiations (Mir A. H., Peuget S., Toulemonde M., Bulot P., Jegou C. et al. 2015). These structural modifications and the formation of other point defects and changes in ring size distribution under α-irradiation that have also been reported may explain why irradiated borosilicate glasses are more reactive with water than pristine glasses (Tribet M., Mir A.H., Gillet C., Jegou C., Mougnaud S et al. 2020).

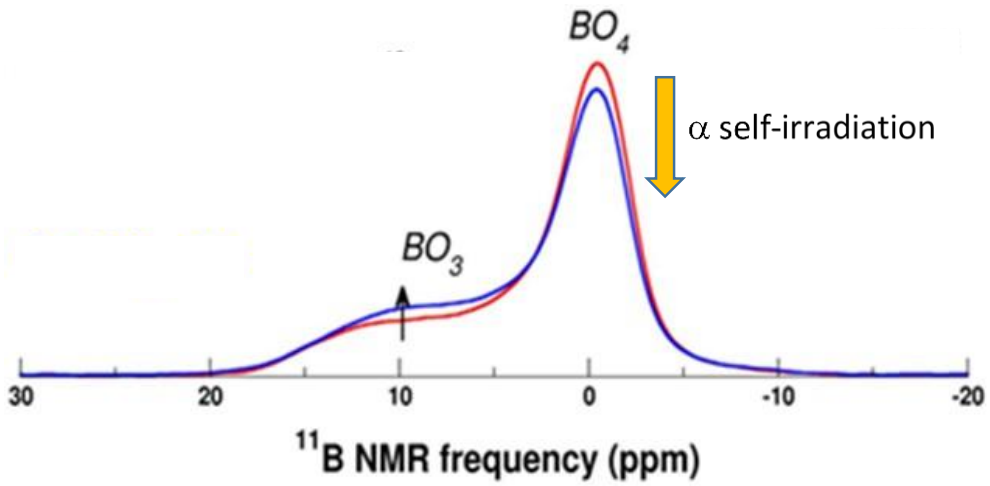

Figure 20. Comparison between the ^{11}B MAS NMR spectra (9.4 T) of a damaged (in blue) and annealed (in red) ^{244}Cm doped (0.13 mol% Cm_2O_3) borosilicate ISG glass. The damaged glass has accumulated an α-decays dose of $4.4x10^{18}\alpha.g^{-1}$ equivalent to 10^4 years of disposal and the annealed glass has accumulated an α-decays dose of $7x10^{16}\alpha.g^{-1}$. (Modified from Charpentier T., Martel L., Mir A. H., Somers J., Jégou C. and Peuget S. (2016) Self-healing capacity of nuclear glass observed by NMR spectroscopy. *Sci. Rep.* **6**, 25499. p. 2. Authorized by Springer Nature)

Resistance of nuclear glasses against alteration in aqueous environment

As any material, glasses chemically react with their environment and degrade over a long period of time. As oxide materials, the main "corroding" agent of glasses is water, either in vapor or in liquid state. This chemical degradation is an issue to all glasses and glass applications, such as natural glasses, commercial glasses and glasses of the cultural heritage. In the case of nuclear waste glasses, the central question is that of the kinetics: at which rate the glass will degrade into the alteration products and release the radioactive nuclei? It is considered that once the glass has degraded, the radiotoxic elements are released from this first barrier, then their containment relies on the other barriers (Vernaz E., Gin S. and Veyer C. 2012). The degradation

by water, or aqueous alteration, is the only process leading to the breakdown of the containment properties, as the other evolution processes such as crystallization may occur on a considerably longer period of time (Fig. 8).

Water reacts with glass by hydration and ionic exchange (1), and hydrolysis (2) (Grambow B. and Müller R. 2001, Conradt R. 2008). Glass hydration and ionic exchange do not modify the glass structure, they produce a "hydrated glass" bearing molecular water and Si-OH (silanol) groups in place of the Si-OM groups where M are cations exchangeable with H^+, such as alkalis and alkaline-earth ions.

$$Si - O - Na + H^+ \leftrightarrow Si - OH + Na^+ \qquad (1)$$

Hydrolysis is the nucleophilic, or acid-base reaction of water with the M-O bonds that breaks these bonds and produce solvated M species (M is any element bound to oxygen). The multi-step hydrolysis of the M-O bonds that form the glass network (M = Si, Al, B…), leads to the destabilization and dissolution of the glass material.

$$Si - O - M + H_2O \leftrightarrow Si - OH + M - OH \qquad (2)$$

Every hydrolysis reaction has an equilibrium constant $K_{eq,M}(T)$ that controls the amount of element M to be dissolved at a given temperature T and at equilibrium. Every hydrolysis reaction also has a kinetic rate $R_{M,T}(t)$ that is the initial rate $R_{M,T,0}$ weighted by the affinity factor.

$$K_{eq,M}(T) = \exp\left(-\frac{\Delta G_M^0(T)}{RT}\right)$$

$$R_{M,T}(t) = R_{M,T,0}\left(1 - \frac{Q_M(t)}{K_{eq}(T)}\right)$$

Where $Q_M(t)$ is the reaction product of the hydrolysis of M at time t and $R_{M,T,0}$ is the initial rate. In multicomponent glasses such as nuclear glasses, all components have different solubilities, all varying differently with the pH. The dissolution is then generally non-congruent, producing an alteration layer at the interface between the pristine glass and the solution, which contains the most insoluble components. For instance, alkalis and boron pass into solution, while Zr, Al (charge-compensated by Ca (Angeli F., Boscarino D., Gin S., Della Mea G., Boizot B. et al. 2001)), Fe, La, Mg, Ca generally stay completely or partially in the silicate alteration gel (depending on the pH) (Molières E., Angeli F., Jollivet P., Gin S., Charpentier T. et al. 2013). Moreover, the material dissolution is irreversible because the reverse reactions cannot back-produce the starting glass. Because of its low solubility and structural role as main network

former, the dissolution rate of the glass is considered as limited by the dissolution rate of SiO_2. The affinity term controlling the kinetics is then the equilibrium with SiO_2 as amorphous silica (or as cristobalite in some geochemical models).

An important experimental approach is to measure the glass dissolution kinetics in static conditions (representative of the deep disposal condition) in various conditions of T, S/V (S surface of exposed glass, V volume of the solution), pH and solution composition. The solution is sampled at regular intervals and analysed by ICP-OES. From the measured concentrations $c_i(t)$, the normalized leached fractions in every element are calculated by:

$$NL_i(t) = \frac{C_i(t) \times V}{x_i \times m \times \Sigma}$$

Where V is the volume of the solution, x_i is the mass fraction of element i in the glass composition, m is the mass of glass powder engaged in the experiment and Σ is the specific surface of the glass powder (in $m^2.g^{-1}$). Then, $NL_i(t)$ is in $g.m^{-2}.d^{-1}$ and represents the amount of dissolved glass considering the amount of element i that has passed into solution. Because B is very rarely found in the alteration layer, it is considered as a good tracer of the dissolution and is used to calculate the glass leached fraction and follow the glass dissolution kinetics (Fig. 14). Following the numerous experimental studies (Cailleteau C., Angeli F., Devreux F., Gin S., Jestin J. et al. 2008; Gin S., Beaudoux X., Angéli F., Jégou C. and Godon N. 2012), the glass dissolution rate in static conditions is divided into three successive regimes: the initial rate, a transition regime, and the residual rate regime (Fig. 21). The initial rate is the dissolution rate in very diluted conditions when no diffusion barrier slows down the kinetics. It is a property of the glass that strongly depends on its composition, on the temperature and on the pH of the solution (Frugier P., Gin S., Minet Y., Chave T., Bonin B. et al. 2008). Secondary influencing parameters are the glass structure (Angéli F., Charpentier T., Jollivet P., de Ligny D., Bergler M. et al. 2018, Mascaraque N., Bauchy M. and Smedskjaer M. M. 2017) and the chemistry of the solution such as its ionic strength (Icenhower J. P. and Dove P. M. 2000) and the presence of complexing species (Tournié A., Majérus O., Lefèvre G., Rager M.-N., Walmé S. et al. 2013). The transition regime corresponds to the progressive drop of the dissolution rate by several orders of magnitude, which has two origins: the saturation of the solution with silica (affinity term Q/K_{eq} approaching 1) and the formation of an alteration layer or sub-layer with diffusion barrier properties (passivating layer). This alteration layer ends up in turn transforming into more stable products. At some time, an almost stationary regime establishes, when the diffusion rate of the reactive species through the passivating layer equals the rate of transformation of this layer into other, less passivating, products. This residual rate regime

corresponds to the slow dissolution and transformation of the glass into a hydrated, porous silicate gel modified with other insoluble products (as Zr and some amount of Al, La, Ca…). It can last a very long time, but it is also possible that at some moment, by exceeding some solubility product and/or induction time, a more insoluble and non-passivating Si-bearing product precipitates, which may take the control of the kinetics and resume the dissolution of the glass by destroying the passivating layer (Fig. 21). This resumption regime has been observed in specific conditions of high pH and/or temperature, caused by the formation of zeolite phases (Fournier, M., Gin, S. and Frugier, P. 2014).

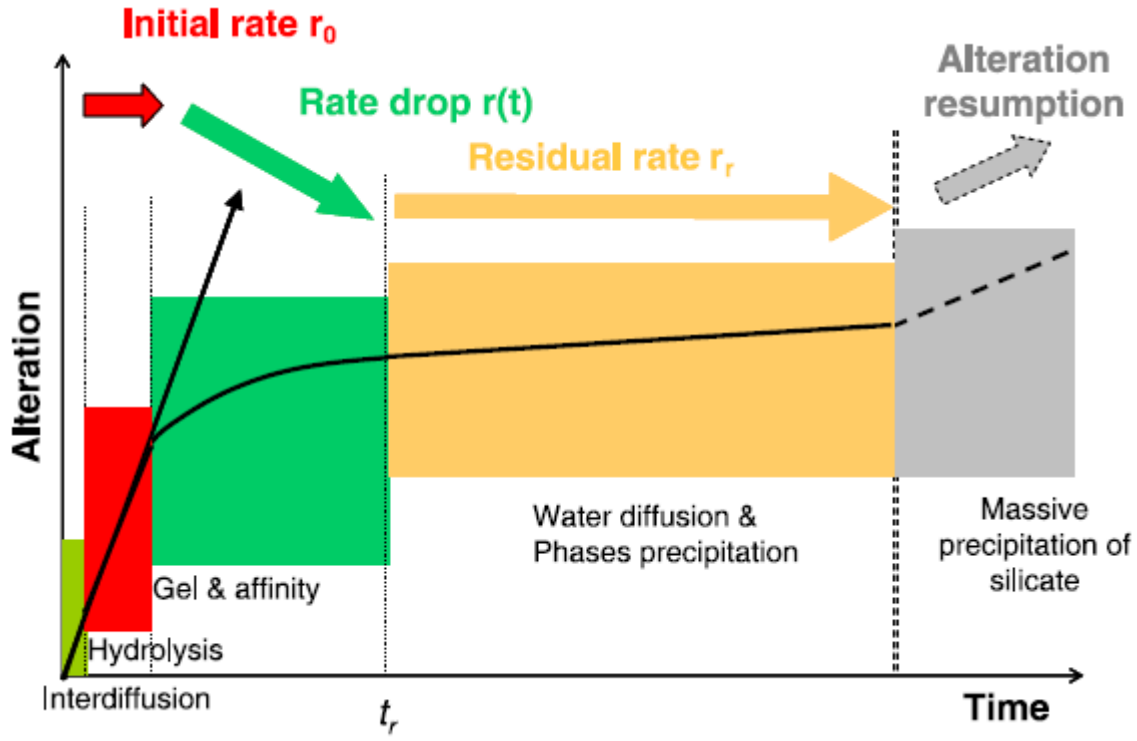

Figure 21. The three successive regimes of the dissolution rate in water of a nuclear borosilicate glass in static conditions: the initial rate, the transition regime, and the residual rate regime. The duration of these different regimes depends on both glass composition and alteration conditions. In specific conditions, a resumption regime can be observed for long times, due to silicate phases precipitation that may affect the passivating power of the alteration layer. (Gin, S., Beaudoux, X., Angéli, F., Jégou, C. and Godon, N. (2012) Effect of composition on the short-term and long-term dissolution rates of ten borosilicate glasses of increasing complexity from 3 to 30 oxides. *J. Non Cryst. Solids* **358**, 2559-2570. p 2665. Reproduced with permission from Elsevier)

The most extensive studies have been undertaken on the SON68 glass (inactive version of the R7T7 French nuclear glass). In a closed system composed of (initially) pure water at 50°C, the assessed residual rate of the SON68 glass is about 5.10^{-5} $g.m^{-2}.d^{-1}$, that is about 7 nm/year (Frugier P., Gin S., Minet Y., Chave T., Bonin B. et al. 2008). This temperature of 50°C is considered representative of the actual temperature of the surface of the glass canisters on a

very long time. The surface microstructure of a SON68 glass altered for 25 years in slowly flowing water equilibrated with granite, sand and (Ni,Cr) corrosion products, at 90°C and 100 bars, is depicted in Fig. 22 (Gin S., Guittonneau C., Godon N., Neff D., Rebiscoul D. et al. 2011). The alteration layer is composed of a hydrated glass, a porous gel and crystalline phyllosilicate phases in the outer part of the gel and on the surface. The dense layer that bears the passivating properties is located at the interface between the pristine glass and the hydrated glass, its diffusion coefficient is about 10^{-21} $m^2.s^{-1}$ characterizing a dense, solid phase.

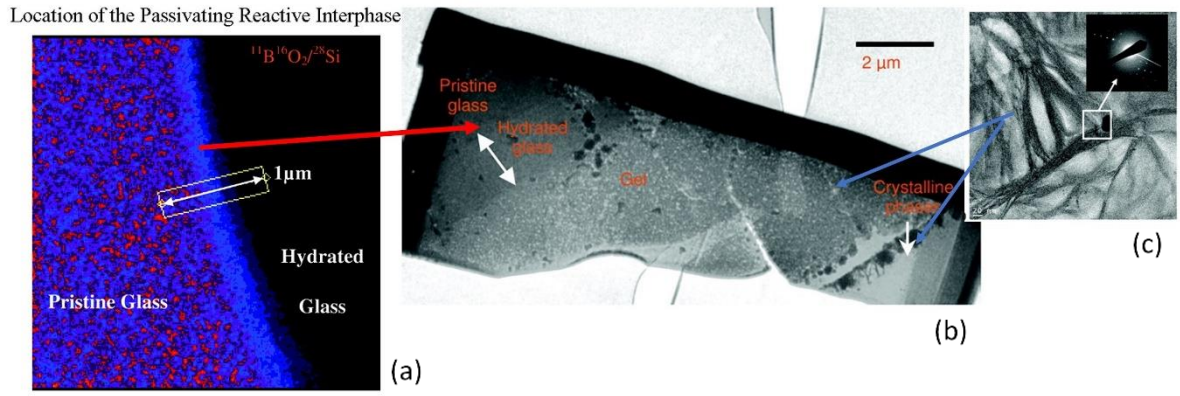

Figure 22. Microstructure of the alteration layer of the SON68 inactive French nuclear borosilicate glass altered for 25 years at 90°C and 100 bars in a confined granitic medium. (a) NanoSIMS analysis of the interface between the pristine glass and the hydrated glass showing a 200 nm thick dense layer. The diffusion coefficient of boron through this layer is of the order 10^{-21} $m^2.s^{-1}$ (b) TEM bright-field image of a FIB cross-section of the altered glass surface, showing the pristine glass and the alteration layer divided into a hydrated glass, a porous silicate gel and a top layer of phyllosilicates (phyllosilicates are also found in the porous gel). (c) TEM bright-field image of the phyllosilicates with an electronic diffraction pattern of a crystallized grain. (Gin S., Guittonneau C., Godon N., Neff D., Rebiscoul D., Cabié M., Mostefaoui S. (2011) Nuclear glass durability: New insight into alteration layer properties. *J. Phys. Chem. C.* **115** 18696-18706. p 18689, 18701 and 18702. Authorized by The American Chemical Society)

Because of the nonlinear time and temperature dependency of the various reaction rates, and because of the coupling of these rates with transport processes through an evolving layer, there is no general theory to predict the kinetics of the dissolution, nor the nature, stability, and properties of the alteration layer. Predictions on the long-term can only be made based on geochemical models using parameters (equilibrium constants, kinetic parameters, diffusion coefficients) determined experimentally on a given glass-environmental system (Frugier P., Gin S., Minet Y., Chave T., Bonin B. et al. 2008, Verney-Carron A., Gin S., Frugier P. and Libourel G. 2010). Archaeological glasses or natural glasses altered for very long time in specific, stable conditions are used to validate the prediction capacities of these models (Verney-Carron A., Gin S. and G. Libourel 2008, Parruzot B., Jollivet P., Rébiscoul D. and Gin S. 2015).

Recently, new mechanisms of glass dissolution and transformation at the interface between the pristine glass and the gel layer have been proposed, following dissolution mechanisms observed for silicate minerals (the coupled interface dissolution-precipitation model, CIDP (Hellmann R., Cotte S., Cadel E., Malladi S., Karlsson L. S. et al. 2015)). The development of analytical techniques with high spatial resolution, such as the atomic probe tomography (APT) and advanced TEM techniques, as well as the use of isotopic tracers have allowed to progress into the understanding of the chemical and microstructural evolution of the alteration layer and of its diffusion properties (Gin S., Jollivet P., Barba Rossa G., Tribet M., Mougnaud S. et al. 2017). Particular attention has been drawn to the effect of environmental parameters such as the presence of iron corrosion products coming from the steel canister, or the composition of the groundwater (De Echave T., Tribet M., Jollivet P., Marques C., Gin S. et al. 2018). For instance, concerning the SON68 borosilicate glass, the presence of Fe^{2+} ions in the anoxic water (Michelin A., Burger E., Rebiscoul D., Neff D., Bruguier F. et al. 2013), or the presence of Mg^{2+} ions (as in the groundwater of the Callovo-Oxfordian site envisaged for the disposal of the French nuclear glass (Grambow B. 2016)) cause the precipitation of Fe-silicate or Mg-smectite phases (Thien, B. M. J., Godon, N., Ballestero, A., Gin, S. and Ayral, A. 2012), which limit the dissolution rate drop by hindering the formation of a dense passivating layer.

In the scenario of the long-term evolution of the French disposal site established by ANDRA (Grambow B. 2016), the nuclear glass will be first exposed to water in the vapor state, for a long period of time of several thousands of years, because of the hydrogen pressure produced by the anoxic corrosion of the steel canisters (Narayanasamy S., Jollivet P., Godon N., Angeli F., Gin S. et al. 2019). The alteration of the glass in vapor state is specific and cannot be confused with the glass alteration in liquid water at high S/V. Water in vapor state or in the film adsorbed onto the glass surface has not the same dynamics and solvation properties as water in "bulk" liquid state. Moreover, the elements dissolved from the glass are not diluted in a liquid phase, so that the precipitation of secondary phases is rapid, modifying the glass surface chemistry (Majérus O., Lehuédé P., Biron I., Alloteau F., Narayanasamy S. et al. 2020). Further research is necessary to improve the understanding of the glass alteration in these specific conditions.

Glass-ceramic wasteforms

For a long time, the presence of crystals in nuclear glasses was regarded as undesirable because of the modification they may induce on the composition and durability against water of the surrounding glass and on the melting process, but now there is a general trend to accept partial

crystallization for some waste if the containment of the final wasteform remains acceptable (Jantzen, C. M. and Ojovan, M. I. 2019). Many studies have been performed to develop nuclear wasteforms consisting of a glassy phase and one or more crystalline phases able to incorporate non-separated HLW or separated long-lived wastes in their structure (Donald I. W. 2016, Caurant D. 2017, McCloy, J.S. and Goel A. 2017). In the general case, such matrices made of crystals dispersed in a more or less abundant glassy phase are called glass composite materials (GCM) (Lee W. E., Ojovan, M. I., Stennett M. C. and Hyatt N. C. 2006). This is the case for instance of high waste loading wasteforms within which uncontrolled melt crystallization may occur during natural cooling of the melt (Figs. 4 and 23).

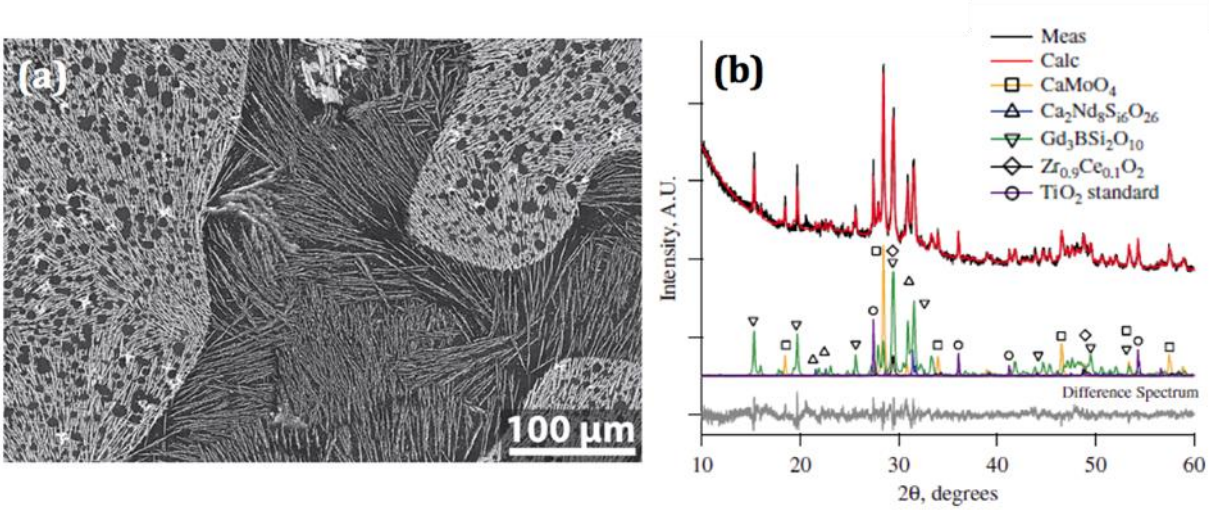

Figure 23. Multi-phase crystallization occurring during the cooling of an aluminoborosilicate melt containing 42 wt% simulated nuclear waste. (a) SEM image (back-scattered electrons) putting in evidence a large scale phase separation in the liquid followed by crystallization in the two phases. (b) X-ray diffraction pattern of the glass-ceramic presented in (a) with identification of the crystalline phases. (Crum J. V., Turo L., Riley B, Tang M. and Kossoy A. (2012) Multi-phase glass-ceramics as a waste form for combined fission products: alkalis, alkaline earths, lanthanides, and transition metals. J. Am. Ceram. Soc. 95, 1297-1303. p. 5. Reproduced with permission from John Wiley and Sons)

Glass-ceramics wasteforms correspond to a particular type of GCM containing small and numerous crystals homogeneously dispersed in a glassy phase that are obtained after controlled heat treatment of a glass containing the waste (nucleation + growth stages) (Fig. 24a) or controlled cooling of a melt, in order to produce a matrix with desired microstructure and crystalline phases in a durable residual glass. These crystalline phases are generally chosen according to their durability and their capacity to incorporate particular categories of elements present in the waste, such as long-lived radionuclides. Similar kind of matrices made of a durable glassy phase and homogeneously dispersed crystals of desired nature and size can also

be obtained by sintering a mixture made of a glass powder and a crystalline phase already containing a particular category of elements present in HLW (encapsulation) (Fig. 24b).

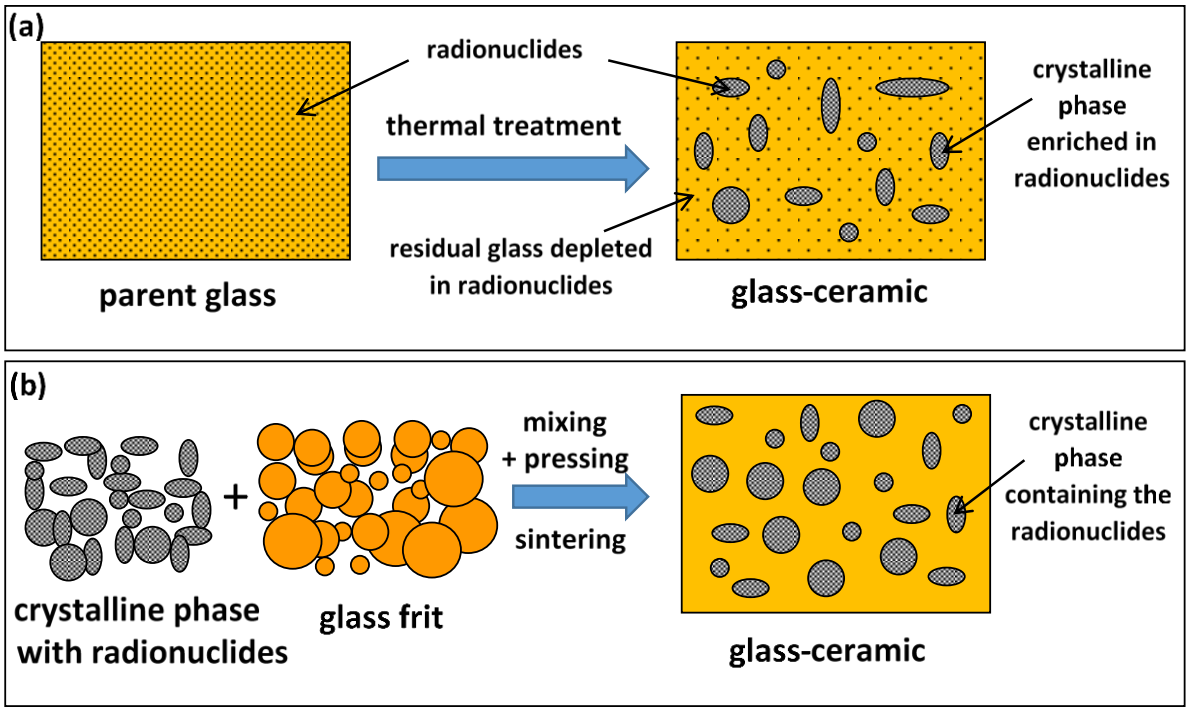

Figure 24. Principle of the specific immobilization of long-lived radionuclides in a glass-ceramic wasteform prepared by crystallization (nucleation + growth) of a glass (referred to as parent glass) containing the radionuclides (a) or by sintering a mixture of powders made of a glass frit and crystals in which are already incorporated the radionuclides (b).

The motivations of the studies on glass-ceramics for waste containment are varied:

- Improvement of mechanical properties, thermal stability and chemical durability in comparison with glassy waste forms.

- Research of more efficient and highly durable matrices than glasses to contain specifically separated long-lived radionuclides in a highly durable crystalline phase (acting as first containment barrier) itself dispersed in a durable residual glass that can be considered as the second barrier against wasteform dissolution by water (Fig. 24a). In the case where the wastes to immobilize are not completely pure (for example actinide-rich waste with some fission products or other elements), the presence of the residual glass can be efficient to immobilize impurities.

Historically, in the 1970s, the first glass-ceramics which have been considered to contain nuclear wastes were prepared by heat treatment of glasses and the initial motivation was only to improve the mechanical and thermal properties of borosilicate glassy wasteforms (Donald I. W., Metcalfe B. L. and Taylor R. N. J. 1997). The first complete work conducted on glass-

ceramic matrices for containment of non-separated wastes was carried out in the 1980s on glass-ceramics containing $CaTiSiO_5$ (titanite) crystals dispersed within an aluminosilicate glassy matrix synthesized by nucleation and growth heat treatment of a glass containing TiO_2 (titanite is a mineral phase known for its capacity to incorporate actinides in its structure and to exhibit good chemical durability) (Hayward P. J. 1988). More recently, several works have been performed on glass-ceramics containing zirconolite ($CaZrTi_2O_7$) crystals for the containment of separated MA that can be specifically isolated from HLW solutions by enhanced separation processes (Loiseau P., Caurant D., Baffier N., Mazerolles L. and Fillet C. 2004, Caurant D., Majérus O., Loiseau P., Bardez I., Baffier N. et al. 2006). In this case, the aim was to obtain after thermal treatment (nucleation + growth, Fig. 25) of a calcium aluminosilicate glass of suitable composition containing ZrO_2, TiO_2 and MA surrogates (Ln), a wasteform acting as a double containment barrier for MA, with the objective of accommodate as much MA as possible in the zirconolite crystals (high partition coefficient) (Figs. 24a and 26). In the ideal case, the parent glass composition should be chosen such that the nucleation rate of the crystalline phase in the bulk is very high (to promote internal crystallization rather than crystallization from the surface) and that the partition coefficient of radionuclides between the crystalline phase and residual glass is high. In the case of the zirconolite-based glass-ceramics, the amount of crystalline phase and the partition coefficient of Ln between zirconolite crystals and the residual glass could be controlled by acting on the parent glass composition, for instance on the Al_2O_3 content (Fig. 26). Nevertheless, in spite of several composition changes performed for this system, a significant amount of Ln always remains in the residual glass and therefore does not benefit from a double containment barrier (Loiseau P., Caurant D., Majérus O. and Baffier N. 2003, Caurant D., Loiseau P., Bardez I. and Gervais C. 2007).

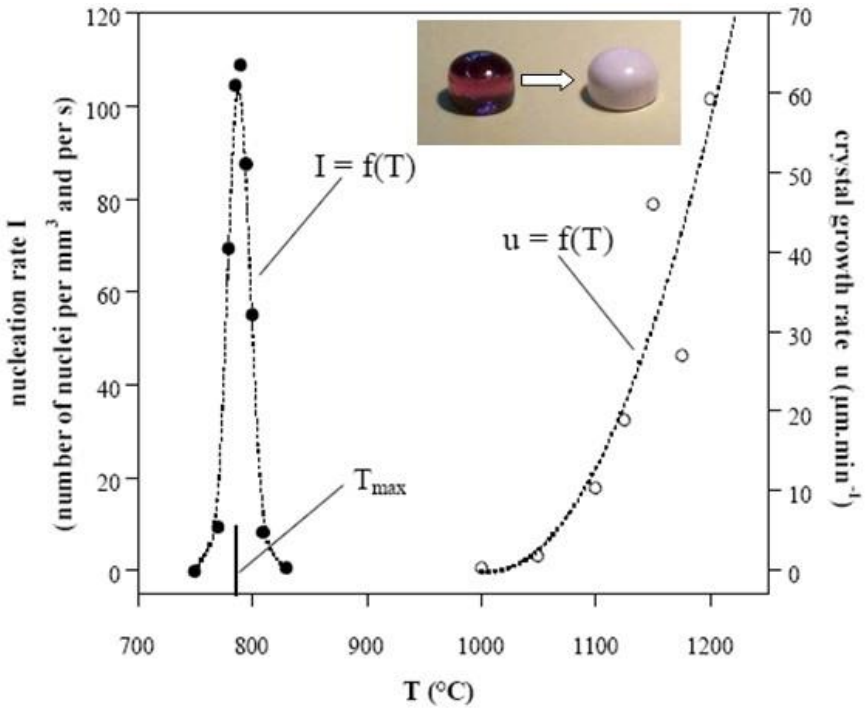

Figure 25. Nucleation (I = f(T)) and crystal growth rate (u = f(T)) curves of zirconolite ($CaZrTi_2O_7$) crystals in the bulk of a calcium aluminosilicate glass bearing ZrO_2 and TiO_2 and leading to zirconolite-based glass-ceramics (Fig. 24). I and u curves are well separated which limits crystallization during melt cooling and allows to control the preparation of glass-ceramics using a two-step thermal treatment (the picture given at the top of the figure shows the transformation of a Nd-doped glass into a glass-ceramic).

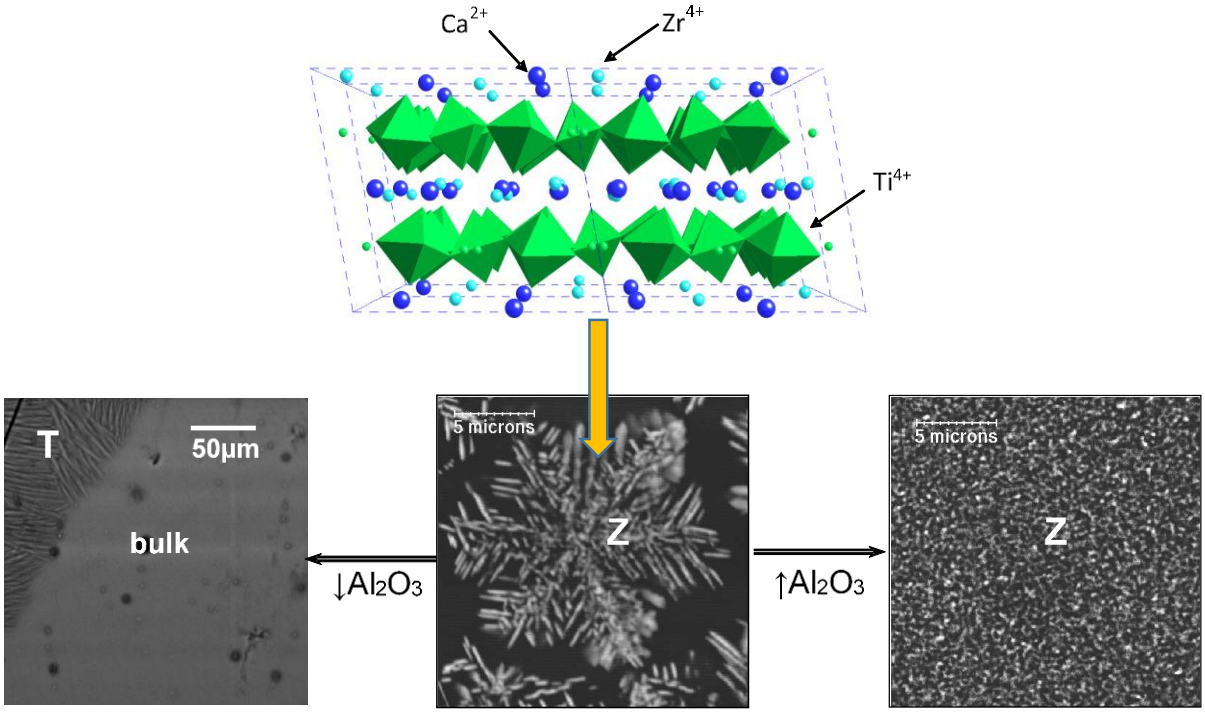

Figure 26. Evolution of the density of zirconolite crystals (Z) formed in the bulk of a glass-ceramic as a function of the variation of Al_2O_3 content (± 2.7 mol%) in a calcium aluminosilicate parent glass bearing ZrO_2 and TiO_2

(T : titanite crystals ($CaTiSiO_5$) growing from glass surface). Glass-ceramics were prepared by a double heat treatment: nucleation at 810°C (2h) and growth at 1050°C (2h). Acting on the Al_2O_3 content in the parent glass strongly affects the zirconolite crystallization rate which can be explained by a competition between Al^{3+}, Ti^{4+} and Zr^{4+} for charge compensators in favor of Al^{3+} that destabilizes Ti^{4+} and Zr^{4+} and promotes zirconolite ($CaZrTi_2O_7$) crystallization (Modified from Caurant D., Loiseau P., Bardez I. and Gervais C. (2007) Effect of Al_2O_3 concentration on zirconolite ($Ca(Zr,Hf)Ti_2O$) crystallization in (TiO_2,ZrO_2,HfO_2)-rich SiO_2-Al_2O_3-CaO-Na_2O glasses. *J. Mater. Sci.* **42**, 8558-8570. p. 8565. Permission from Springer Nature). The zirconolite structure is shown at the top of the figure (MA^{3+} and Ln^{3+} can substitute for Ca^{2+} and Zr^{4+} with adapted compensation charge schemes).

One alternative way to increase the partitioning ratio of the waste between the glass and the crystals is to prepare a wasteform not by crystallization of a glass already containing the waste as in glass-ceramics (Fig. 24a), but by encapsulating a highly durable crystalline phase containing the waste (prepared independently in a first stage) in a durable glass by sintering a mixture of two powders with adapted particle sizes (Figs. 24b). For instance, actinide wasteforms prepared by encapsulating highly durable pyrochlore ($Gd_2Zr_2O_7$, $La_2Zr_2O_7$) particles in a borosilicate or lead silicate glass have been proposed (Fig. 27). (Pace S., Cannillo V., Wu J., Boccaccini D. N., Seglem S. et al. 2005, Boccaccini A. R., Berthier T. and Seglem S. 2007)

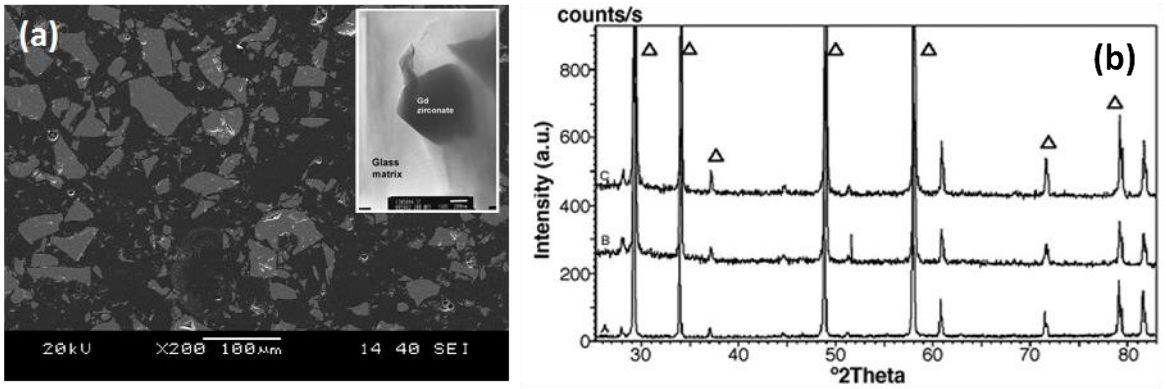

Figure 27. (a) SEM image of a $Gd_2Zr_2O_7$ pyrochlore-based borosilicate GCM wasteform obtained by encapsulation by sintering under pressure (5 MPa) at 620°C (2h) a mixture made of $Gd_2Zr_2O_7$ and borosilicate glass powders. The TEM image given at the top right of the SEM image shows the absence of reaction between pyrochlore crystals and the glassy matrix during sintering. (b) XRD patterns of the $Gd_2Zr_2O_7$ powder (bottom) and of the glass + $Gd_2Zr_2O_7$ (30 vol%) mixture sintered at 650°C in atmosphere (middle) or under pressure (top) showing only the pyrochlore XRD lines. (Boccaccini A. R., Berthier T. and Seglem S. (2007) Encapsulated gadolinium zirconate pyrochlore particles in soda borosilicate glass as novel radioactive waste form. *Ceram. Int.* **33**, 1231-1235. p. 1233. Reproduced with permission from Elsevier)

In all cases, the choice of the crystalline phase in which one expect to incorporate the radionuclides is generally based on results from literature: knowledge of natural and highly durable crystalline phases (natural analogues) having incorporated natural radionuclides (U, Th), studies on single-phase ceramics able to incorporate radionuclides and exhibiting very good long-term containment properties as demonstrated by leaching and irradiation tests.

In comparison with nuclear glasses, such GCM prepared either by the classical glass-ceramic technology (melting of a glass + crystallization thermal treatment) or by encapsulation (grinding + sintering) remain more complicated to synthesize than nuclear glasses, because of additional steps that can be difficult to achieve in a radioactive environment. Nevertheless, studies continue around the world on this type of matrices constituted of a highly durable crystalline phase able to incorporate actinide-rich waste dispersed in a glass (Liao C-Z., Liu C., Su M. and Shih K. 2017, Kong L., Wei T., Zhang Y. and Karatchevtseva I. 2018). Moreover, the concept of double containment barrier in glass-ceramic wasteforms is also envisaged to increase the efficiency of the immobilization of non-radioactive hazardous waste in comparison with homogeneous glassy wasteforms (Caurant D. 2007). This is the case for instance for chromium-rich industrial waste for which the possibility to prepared spinel-based glass-ceramics with a high partitioning ratio of chromium in the spinel ($MgCr_xAl_{2-x}O_4$) crystals has be demonstrated (Liao C., Tang Y., Liu C., Shih K. and Li F. 2016).

Conclusions

About 70 years after the first studies on nuclear waste vitrification and more than 40 years after the start of industrial vitrification, oxide glasses - and mainly borosilicate ones - always remain the only host used to incorporate high level radioactive waste (HLW) from commercial and defense sources despite the many works that have been carried out on ceramic matrices. Their great structural flexibility, allowing them to accommodate almost all the elements present in the waste resulting from spent nuclear fuel reprocessing, their good self-irradiation resistance and chemical durability associated with their ease of fabrication by melting and casting explain the success of glassy wasteforms still today. Vitrification is now used in many countries around the world with constant improvements and the development of new types of melters.

Since the start of vitrification, a large number of works have been carried out to adapt glass formulation to the evolution of waste composition, with an increasingly precise knowledge of the structure and properties of nuclear glasses, and in particular of the way the various elements present in the waste are incorporated into the glassy network and how this incorporation can be optimized by adapting the composition of the glass. Very extensive studies are still in progress

in order to understand and to model the long-term behavior of nuclear glasses during their geological storage (alteration mechanisms in submerged aqueous medium or in the presence of water vapor, impact of internal irradiation on glass structure and properties). For a long time, the presence of crystals in nuclear glasses was regarded as undesirable because of the modification they may induce on their properties and on their impact on the melting process, but now there is a general trend to accept partial crystallization for some waste if the containment of the final wasteform remains acceptable, leading to glass composite materials (GCM). Belonging to this family of wasteforms, glass-ceramics that can obtained by controlled crystallization of a glass bearing radionuclides can be envisaged for instance to immobilize actinide-rich waste.

The building of new nuclear power stations around the world with possible spent fuel reprocessing will lead in the future to an increasing need for waste vitrification. Moreover, the emergence of new HLW of various compositions coming for instance from the decommissioning and dismantling of old nuclear facilities and, in a more distant future, of new types of waste coming from new generations of nuclear power reactors requiring reprocessing of the spent fuel will still require many studies on new nuclear glass compositions for their immobilization.

Further reading

Caurant D., Loiseau P., Majérus O., Aubin-Chevaldonnet V., Bardez I. and Quintas A. (2009) Glasses, glass-ceramics and ceramics for immobilization of highly radioactive nuclear wastes. Nova Science Publishers, Hauppauge, New York (USA).

Donald I. W. (2010) Waste immobilization in glass and ceramic based hosts. Radioactive, toxic and hazardous wastes. Wiley, Chichester (UK).

Ojovan M. I. (2011) Handbook of advanced radioactive waste conditioning technologies. Woodhead Publishing Series in Energy: Number 12. Woodhead Publishing Limited, Cambridge (UK).

Ojovan M. I., Lee W. E. and Kalmykov S. N. (2019) An introduction to nuclear waste immobilisation. 3rd Edition Elsevier, Oxford (UK).

List of relevant web pages

About deep geological disposal facility in France for radioactive waste:

https://international.andra.fr/solutions-long-lived-waste/cigeo

About nuclear fuel cycle and vitrification plants in the US and in France:

https://www.youtube.com/watch?v=YaJ8SU4OCz4

https://www.youtube.com/watch?v=V0UJSlKIy8g

About the nuclear fuel cycle:

https://www.nuclear-power.net/nuclear-power-plant/nuclear-fuel/nuclear-fuel-cycle/open-fuel-cycle-vs-closed-fuel-cycle/

https://www.world-nuclear.org/information-library/nuclear-fuel-cycle/introduction/nuclear-fuel-cycle-overview.aspx

References

Angeli F., Boscarino D., Gin S., Della Mea G., Boizot B., Petit J. C. (2001) Influence of calcium on sodium aluminosilicate glass leaching behaviour. *Phys. Chem. Glas.* **42**, 279-286.

Angeli F., Charpentier T., Gaillard M. and Jollivet P. (2008) Influence of zirconium on the structure of pristine and leached soda-lime borosilicate glasses: Towards a quantitative approach by ^{17}O MQMAS NMR. *J. Non-Cryst. Solids* **354**, 3713-3722.

Angeli F., Charpentier T., Molières E., Soleilhavoup A., Jollivet P. and Gin S. (2013) Influence of lanthanum on borosilicate glass structure: A multinuclear MAS and MQMAS NMR investigation. *J. Non-Cryst. Solids* **376**, 189-198.

Angeli F., Charpentier T., Jollivet P., de Ligny D., Bergler M., Veber A., Gin S. and Li H. (2018) Effect of thermally induced structural disorder on the chemical durability of International Simple Glass. *npj Mater. Degrad.* **2,** 31.

Aubin-Chevaldonnet V., Caurant D., Dannoux A., Gourier D., Charpentier T., Mazerolles L. and Advocat T. (2007) Preparation and characterization of $(Ba,Cs)(M,Ti)_8O_{16}$ ($M = Al^{3+}$, Fe^{3+}, Ga^{3+}, Cr^{3+}, Sc^{3+}, Mg^{2+}) hollandite ceramics developed for radioactive cesium immobilization. *J. Nucl. Mater.* **366**, 137-160.

Bardez I. (2004) Study of the structural characteristics and properties of glasses rich in rare earths intended for the immobilization of fission products and long-lived elements (in French). PhD of the University Pierre and Marie Curie. Paris, France. https://pastel.archives-ouvertes.fr/pastel-00001075

Bardez-Giboire I., Kidari A., Magnin M., Dussossoy J-L., Peuget S., Caraballo R., Tribet M., Doreau F. and Jegou C. (2017) Americium and trivalent lanthanides incorporation in high-level waste glass-ceramics. *J. Nucl. Mater.* **492**, 231-238.

Bates J. K., Seitz M. G. and Steinler M. J. (1984) The relevance of vapor phase hydration aging to nuclear waste isolation. *Nucl. Chem. Waste Manag.* **5**, 63-73.

Boccaccini A. R., Berthier T. and Seglem S. (2007) Encapsulated gadolinium zirconate pyrochlore particles in soda borosilicate glass as novel radioactive waste form. *Ceram. Int.* **33**, 1231-1235.

Bohre A., Avasthi K. and Pet'kov V. I. (2017) Vitreous and crystalline phosphate high level waste matrices: Present status and future challenges. *J. Ind. Eng. Chem.* **50**, 1-14.

Bonin B. (2008) Treatment and recycling of spent nuclear fuel. Actinide partitioning - Application to waste management. In Bonin B., Bouquin B., Dozol M., Lecomte M. and Forestier A. (eds.). Commissariat à l'énergie atomique. Gif-sur-Yvette : A Nuclear Energy Division Monograph. https://www.cea.fr/english/Pages/resources/nuclear-energy-monographs/treatment-recycling-spent-nuclear-fuel.aspx

Boullis B. and Devezeaux de Lavergne J-G. (2006) The treatment of spent fuel: a well-controlled sector (in French). *Clefs CEA* **53**, 19-25.

Brehault A., Patil D., Kamat H., Youngman R. E., Thirion L. M., Mauro J. C., Corkhill C. L., McCloy J. S. and Goel A. (2018) Compositional dependence of solubility/retention of molybdenum oxides in aluminoborosilicate-based model nuclear waste glasses. *Phys. Chem. B.* **122**, 1714-1729.

Bridge B. and Patel N. D. (1986) The elastic constants and structure of the vitreous system Mo-P-O. *J. Mater. Sci.* **21**, 1187-1205.

Cachia J.-N., Deschanels X., Den Auwer C., Pinet O., Phalippou J., Hennig C. and Scheinost A. (2006) Enhancing cerium and plutonium solubility by reduction in borosilicate glass. *J. Nucl. Mater.* **352**, 182-189.

Cailleteau C., Angeli F., Devreux F., Gin S., Jestin J., Jollivet P. and Spalla O. (2008) Insight into silicate-glass corrosion mechanisms. *Nat. Mater.* **7**, 978-983.

Calas G., Legrand M., Galoisy L. and Ghaleb D. (2003) Structural role of molybdenum in nuclear glasses: an EXAFS study. *J. Nucl. Mater.* **322**, 15-20.

Cantrel E., Courtadon A., Blanchard S. and Girold C. (2015) Management of HL deposits for the D&D of UP1 reprocessing plant - Retrieval and treatment scenarios. WM 2015 Conference, March 15-19, 2015, Phoenix, Arizona, USA. http://archive.wmsym.org/2015/papers/15295.pdf

Caurant D., Majérus O., Loiseau P., Bardez I., Baffier N. and Dussossoy J-L. (2006) Crystallization of neodymium-rich phases in silicate glasses developed for nuclear waste immobilization. *J. Nucl. Mater.* **354**, 143-162.

Caurant D., Majérus O., Fadel E., Lenoir M., Gervais C. and Pinet O. (2007) Effect of molybdenum on the structure and on the crystallization of SiO_2-Na_2O-CaO-B_2O_3 glasses. *J. Am. Ceram. Soc.* **90**, 774-783.

Caurant D., Loiseau P., Bardez I. and Gervais C. (2007) Effect of Al_2O_3 concentration on zirconolite (Ca(Zr,Hf)Ti_2O) crystallization in (TiO_2,ZrO_2,HfO_2)-rich SiO_2-Al_2O_3-CaO-Na_2O glasses. *J. Mater. Sci.* **42**, 8558-8570.

Caurant D., Quintas A., Majérus O., Charpentier T. and Bardez I. (2008) Structural role and distribution of alkali and alkaline-earth cations in rare earth-rich aluminoborosilicate glasses. *Adv. Mater. Res.* **39-40**, 19-24.

Caurant D., Loiseau P., Majérus O., Aubin-Chevaldonnet V., Bardez I. and Quintas A. (2009) Glasses, glass-ceramics and ceramics for immobilization of highly radioactive nuclear wastes. Hauppauge, New York (USA): Nova Science Publishers.

Caurant D. (2017) Glass-ceramics for waste immobilization. In Neuville D., Cormier L., Caurant D. and Montagne L. (eds.) From glass to crystal. Nucleation, growth and phase separation: from research to applications. pp. 491-526. Les Ullis: EDP Sciences.

Charpentier T., Martel L., Mir A. H., Somers J., Jégou C. and Peuget S. (2016) Self-healing capacity of nuclear glass observed by NMR spectroscopy. *Sci. Rep.* **6**, 25499.

Chen H., Marcial J., Ahmadzadeh M., Patil D. and McCloy J. (2020) Partitioning of rare earths in multiphase nuclear waste glass-ceramics. *Int. J. Appl.Glass Sci.* **11**, 660-675.

Chouard N, Caurant D., Majérus O., Dussossoy J. L., Ledieu A., Peuget S., Baddour-Hadjean R. and Pereira-Ramos J. P. (2011) Effect of neodymium oxide on the solubility of MoO_3 in an aluminoborosilicate glass. *J. Non-Cryst. Solids* **357**, 2752-2762.

Chouard N, Caurant D., Majérus O., Dussossoy J. L., Klimin S. and Pytalev D. (2015) Effect of MoO_3, Nd_2O_3, and RuO_2 on the crystallization of soda-lime aluminoborosilicate glasses. *J. Mater. Sci.* **50,** 219-241.

Chouard N., Caurant D., Majérus O., Guezi-Hasni N., Dussossoy J.-L., Baddour-Hadjean R. and Pereira-Ramos J-P. (2016) Thermal stability of SiO_2-B_2O_3-Al_2O_3-Na_2O-CaO glasses with high Nd_2O_3 and MoO_3 concentrations. *J. Alloy. Compd.* **671**, 84-99.

Chouard N., Caurant D., Majérus O., Dussossoy J.-L., Loiseau P., Grygiel C. and Peuget S. (2019) External irradiation with heavy ions of neodymium silicate apatite ceramics and glass-ceramics. *J. Nucl. Mater.* **516**, 11-29.

Colombo P., Brusatin G., Bernardo E. and Scarinci G. (2003) Inertization and reuse of waste materials by vitrification and fabrication of glass-based products. *Curr. Opin. Solid State Mater. Sci.* **7**, 225-239.

Connelly A. J., Hyatt N. C., Travis K. P., Hand R. J., Stennett M. C., Gandy A. S., Brown A. P. and Apperley D. C. (2013) The effect of uranium oxide additions on the structure of alkali borosilicate glasses. *J. Non-Cryst. Solids* **378**, 282-289.

Conradt R. (2008) Chemical durability of oxide glasses in aqueous solutions: a review, *J. Am. Ceram. Soc.* **91**, 728-735.

Crum J. V., Turo L., Riley B, Tang M. and Kossoy A. (2012) Multi-phase glass-ceramics as a waste form for combined fission products: alkalis, alkaline earths, lanthanides, and transition metals. *J. Am. Ceram. Soc.* **95**, 1297-1303.

De Echave T., Tribet M., Jollivet P., Marques C., Gin S. and Jégou C. (2018) Effect of clayey groundwater on the dissolution rate of SON68 simulated nuclear waste glass at 70 °C. *J. Nucl. Mater.* **503**, 279-289.

Deschanels X., Peuget S., Cachia J. N. and Charpentier T. (2007) Plutonium solubility and self-irradiation effects in borosilicate glass. *Prog. Nucl. Energ.* **49**, 623-634.

Donald I. W., Metcalfe B. L. and Taylor R. N. J. (1997) The immobilization of high level radioactive wastes using ceramics and glasses. *J. Mater. Sci.* **32**, 5851-5887.

Donald I. W. (2007) Immobilisation of radioactive and non-radioactive wastes in glass-based systems: an overview. *Eur. J. Glass Sci. Technol. A* **48**, 155-163.

Donald I. W. (2016) Vitrification of radioactive and hazardous wastes. In The science and technology of inorganic glasses and glass-ceramics. pp 261-300. Sheffield: Society of Glass Technology.

Du J. and Cormack A. N. (2005) The structure of erbium doped sodium silicate glasses. *J. Non-Cryst. Solids* **351**, 2263-2276.

Eller, P. G., Jarvinen J. D., Purson J. D., Penneman R. A., Ryan R. R., Lytle F. W. and Greegor R. B. (1985) *Radiochim. Acta* **39**, 17-22.

Ewing R. C., Whittleston R. A. and Yardley B. W. D. (2016) Geological disposal of nuclear waste: a primer. *Elements* **12**, 233-237.

Fournier, M., Gin, S. and Frugier, P. (2014) Resumption of nuclear glass alteration: state of the art. *J. Nucl. Mater.* **448**, 348-363.

Frugier P., Gin S., Minet Y., Chave T., Bonin B., Godon N., Lartigue J., Jollivet J., Ayral A., Dewindt L. (2008) SON68 nuclear glass dissolution kinetics: Current state of knowledge and basis of the new GRAAL model. *J. Nucl. Mater.* **380**, 8-21.

Gaddam A., Fernandes H. R., Tulyaganov D. U. and Ferreira J. M. F. (2019) The structural role of lanthanum oxide in silicate glasses. *J. Non-Cryst. Solids* **505**, 18‑27.

Galoisy L., Pélegrin E., Arrio M-A., Ildefonse P., Calas G., Ghaleb D., Fillet C. and Pacaud F. (1999) Evidence for 6-coordinated zirconium in inactive nuclear waste glasses. *J. Am. Ceram. Soc.* **82**, 2219-2224.

Gasnier E., Bardez-Giboire I., Montouillout V., Pellerin N., Allix M., Massoni N., Ory S., Cabie M., Poissonnet S. and Massiot D. (2014) Homogeneity of peraluminous SiO_2-B_2O_3-Al_2O_3-Na_2O-CaO-Nd_2O_3 glasses: Effect of neodymium content. *J. Non-Cryst. Solids* **405**, 55-62.

Gin S., Guittonneau C., Godon N., Neff D., Rebiscoul D., Cabié M. and Mostefaoui S. (2011) Nuclear glass durability: New insight into alteration layer properties, *J. Phys. Chem. C.* **115** 18696-18706.

Gin, S., Beaudoux, X., Angéli, F., Jégou, C. and Godon, N. (2012) Effect of composition on the short-term and long-term dissolution rates of ten borosilicate glasses of increasing complexity from 3 to 30 oxides. *J. Non Cryst. Solids* **358**, 2559-2570.

Gin S., Jollivet P., Tribet M., Peuget S. and Schuller S. (2017) Radionuclides containment in nuclear glasses: an overview. *Radiochim. Acta* **105**, 927-959.

Gin S., Jollivet P., Barba Rossa G., Tribet M., Mougnaud S., Collin M., Fournier M., Cadel E., Cabie M. and Dupuy L. (2017) Atom-Probe Tomography, TEM and ToF-SIMS study of borosilicate glass alteration rim: A multiscale approach to investigating rate-limiting mechanisms. *Geochim. Cosmochim. Acta.* **202**, 57-76.

Girold C., Francois S., Petit L., Catherin S., Prevost T., Fourcy E. and Viand A. (2018) French innovative processes in the field of thermal treatment for decommissioning and legacy waste. *Proceedings of the 44th Annual Waste Management Conference (WM2018)*, pp 3074-3087. Phoenix (USA): Waste Management Symposia, Inc. (https://hal-cea.archives-ouvertes.fr/cea-02339255.)

Goel A., McCloy J. S., Windisch C. F., Riley B. J., Schweiger M. J., Rodriguez C. P. and Ferreira J. M. F. (2013) Structure of rhenium-containing sodium borosilicate glass. *Int. J. Appl. Glass Sci.* **4**, 42-52.

Grambow B. (2016) Geological disposal of radioactive waste in clay. *Elements* **12**, 239-245.

Grambow B. and Müller R. (2001) First-order dissolution rate law and the role of surface layers in glass performance assessment. *J. Nucl. Mater.* **298**, 112–124.

Gregg D. J. and Vance E. R. (2016) Synroc tailored waste forms for actinide immobilization. *Radiochim. Acta* **105**, 907-925.

Guy C., Audubert F., Lartigue J-E., Latrille C., Advocat T. and Fillet C. (2002) New conditionings for separated long-lived radionuclides. *C. R. Physique* **3**, 827-837.

Harisson M. T. (2014) Vitrification of high level waste in the UK. *Procedia Mater. Sci.* **7**, 10-15.

Hayward P. J. (1988) The use of glass ceramics for immobilising high level wastes from nuclear fuel recycling. *Glass Technol.: Eur. J. Glass Sci. Technol. A* **29**, 122-136.

Hellmann R., Cotte S., Cadel E., Malladi S., Karlsson L.S., Lozano-Perez S., Cabié M. and Seyeux A. (2015) Nanometre-scale evidence for interfacial dissolution–reprecipitation control of silicate glass corrosion. *Nat. Mater.* **14**, 307-311.

Hench L. L., Clark D. E. and Harker A. B. (1986) Nuclear waste solids. Review. *J. Mater. Sci.* **21**, 1457-1478.

Hrma P., Vienna J. D., Wilson B. K., Plaisted T. J. and Heald S. M. (2006) Chromium phase behavior in a multi-component borosilicate glass melt. *J. Non-Cryst. Solids* **352**, 2114-2122.

Icenhower J. P. and Dove P. M. (2000) The dissolution kinetics of amorphous silica into sodium chloride solutions: Effects of temperature and ionic strength. *Geochim. Cosmochim. Acta.* **64** 4193-4203.

Jantzen C. M. (1986) Systems approach to nuclear waste glass development. *J. Non-Cryst. Solids* **84**, 215-225.

Jantzen C. M., Brown K. G. and Pickett J. B. (2011) Durable glass for thousands of years. *Int. J. Appl. Glass Sci.* **1**, 38-62.

Jantzen C. M. (2011) Development of glass matrices for high level radioactive wastes. In Ojovan M. I. (ed.) Handbook of advanced radioactive waste conditioning technologies. pp 230-292. Cambridge: Woodhead Publishing Ltd.

Jantzen, C. M. and Ojovan, M. I. (2019) On Selection of matrix (wasteform) material for higher activity nuclear waste immobilization (Review). *Russ. J. Inorg. Chem.* **64,** 1611-1624.

Kaspar T. C., Ryan J. V., Pantano C. G., Rice J., Trivelpiece C., Hyatt N. C., Corkhill C. L., Mann C., Hand R. J., Kirkham M. A., Crawford C. L., Jantzen C. M., Du J., Lu X., Harrison M. T., Cushman C., Linford M. R. and Smith N. J. (2019) Physical and optical properties of the International Simple Glass. *npj Mater. Degrad.* **3,** 15.

Kidari A., Dussossoy J-L., Brackx E., Caurant D., Magnin M. and Bardez-Giboire I. (2012) Lanthanum and neodymium solubility in simplified SiO_2-B_2O_3-Na_2O-Al_2O_3-CaO high level waste glass. *J. Am. Ceram. Soc.* **95**, 2537-2544.

Kim D.S., Peeler D.K. and Hrma P. (1995) Effect of crystallisation on the chemical durability of simulated nuclear waste glasses. *Ceram. Bull.* **61**, 177-185.

Kong L., Wei T., Zhang Y. and Karatchevtseva I. (2018) Phase evolution and microstructure analysis of $CaZrTi_2O_7$ zirconolite in glass. *Ceram. Int.* **44**, 6285-6292.

Krishnamurthy A., Nguyen T., Fayek M., Shabaga B. and Kroeker S. (2020) Network structure and dissolution properties of phosphate-doped borosilicate glasses. *J. Phys. Chem. C* **124**, 21184-21196.

Laverov N. P., Yudintsev S. V., Kochkin B. T. and Malkovsky V. I. (2016) The Russian strategy of using crystalline rock as a repository for nuclear waste. *Elements* **12**, 253-256.

Lee W. E., Ojovan, M. I., Stennett M. C. and Hyatt N. C. (2006) Immobilisation of radioactive waste in glasses, glass composite materials and ceramics. *Adv. Appl. Ceram.* **105**, 3-12.

Lemesle T., Méar F. O., Campayo L., Pinet O., Revel B. and Montagne L. (2014) Immobilization of radioactive iodine in silver aluminophosphate glasses. *J. Hazard. Mater.* **264**, 117-126.

Le Losq G., Neuville D. R., Chen W., Florian P., Massiot D., Zhou Z. and Greaves G. N. (2017) Percolation channels: a universal idea to describe the atomic structure and dynamics of glasses and melts. *Sci. Rep.* **7,** 16490.

Liao C., Tang Y., Liu C., Shih K. and Li F. (2016) Double-barrier mechanism for chromium immobilization: A quantitative study of crystallization and leachability. *J. Hazard. Mater.* **311**, 246-253.

Liao C-Z., Liu C., Su M. and Shih K. (2017) Quantification of the partitioning ratio of minor actinide surrogates between zirconolite and glass in glass-ceramic for nuclear waste disposal. *Inorg. Chem.* **56**, 9913-9921.

Loiseau P., Caurant D., Majérus O. and Baffier N. (2003) Crystallization study of (TiO_2,ZrO_2)-rich SiO_2-Al_2O_3-CaO glasses. *J. Mater. Sci.* **38**, 843-852.

Loiseau P., Caurant D., Baffier N., Mazerolles L. and Fillet C. (2004) Glass-ceramic nuclear waste forms obtained from SiO_2-Al_2O_3-CaO-ZrO_2-TiO_2 glasses containing lanthanides (Ce, Nd, Eu, Gd, Yb) and actinides (Th): study of internal crystallization. *J. Nucl. Mater.* **335**, 14-32.

Lu X., Deng L., Kerisit S. and Du J. (2018) Structural role of ZrO_2 and its impact on properties of boroaluminosilicate nuclear waste glasses. *npj Mater. Degrad.* **2,** 19.

Lutze W. (1988) Silicate glasses. In Lutze W. & Ewing R. C. (eds.) Radioactive waste forms for the future. pp 1-159. Elsevier Science Publishers B. V.

Madic C. Lecomte M., Baron P. and Boullis B. (2002) Separation of long-lived radionuclides from high active nuclear waste. *C. R. Physique* **3,** 797-811.

Magnin M. (2009) Study of phase separation and crystallization phenomena in soda-lime borosilicate glass enriched in MoO_3. PhD of the University Pierre and Marie Curie. Paris, France. https://inis.iaea.org/collection/NCLCollectionStore/_Public/42/039/42039802.pdf

Magnin M., Schuller S., Mercier C., Trébosc J., Caurant D., Majérus O., Angéli F. and Charpentier C. (2011) Modification of molybdenum structural environment in borosilicate glasses with increasing content of boron and calcium oxide by ^{95}Mo MAS NMR. J. *Am. Ceram. Soc*. **94**, 4274-4282.

Majérus O., Lehuédé P., Biron I., Alloteau F., Narayanasamy S. and Caurant D. (2020) Glass alteration in atmospheric conditions: crossing perspectives from cultural heritage, glass industry, and nuclear waste management. *npj Mater. Degrad.* **4**, 27.

Malchukova E., Boizot B., Petite G. and Ghaleb D. 2009 Irradiation effects in oxide glasses doped with transition and rare-earth elements. *Eur. Phys. J. Appl. Phys.* **45**, 10701.

Mascaraque N., Bauchy M. and Smedskjaer M. M. (2017) Correlating the network topology of oxide glasses with their chemical durability. *J. Phys. Chem. B.* **121**, 1139-1147.

McKeown D. A, Gan H. and Pegg I. L. (2017) X-ray absorption and Raman spectroscopy studies of molybdenum environments in borosilicate waste glasses. *J. Nucl. Mater.* **488**, 143-149.

McCloy, J.S. and Goel A. (2017) Glass-ceramics for nuclear-waste immobilization. *MRS Bull.* **42**, 233-240.

Meaker T. F., Peeler D. K., Marra J. C., Pareizs J. M. and Ramsey W. G. (1996) Actinide solubility in lanthanide borosilicate glass for possible immobilization and disposition. MRS proceedings vol. 465. Scientific Basis for Nuclear Waste Management. pp. 1281-1286.

Metcalfe B. L. and Donald I. W. (2013) Management of radioactive waste (RAW) from nuclear weapons programmes. In Lee W. E., Ojovan M.I. and Jantzen C. M. (eds) Radioactive waste management and contaminated site clean-up. Processes, technologies and international experience, pp 775-800. Sawston (UK): Woodhead Publishing.

Ménard O., Advocat T., Ambrosi J. P. and Michard A. (1998) Behaviour of actinides (Th, U, Np and Pu) and rare earths (La, Ce and Nd) during aqueous leaching of a nuclear glass under geological disposal conditions. *Appl. Geochem.* **13**, 105-126.

Michelin A., Burger E., Rebiscoul D., Neff D., Bruguier F., Drouet E., Dillmann P. and Gin S. (2013) Silicate glass alteration enhanced by iron: Origin and long-term implications. *Environ. Sci. Technol.* **47**, 750-756.

Mir A. H., Peuget S., Toulemonde M., Bulot P., Jegou C., Miro S. and Bouffard S. (2015) Defect recovery and damage reduction in borosilicate glasses under double ion beam irradiation. *EPL* **112**, 36002.

Molières E., Angeli F., Jollivet P., Gin S., Charpentier T., Majérus O., Barboux P., de Ligny D. and Spalla O. (2013) Chemical durability of lanthanum-enriched borosilicate glass. *Int. J. Appl. Glass Sci.*, **4**, 383-394.

Muller I. and Weber W. J. (2001) Plutonium in crystalline ceramics and glasses. *MRS Bull.* **26**, 698-706.

Muller I. S., McKeown D. A. and Pegg I. L. (2014) Structural behavior of Tc and I ions in nuclear waste glass. *Procedia Mater. Sci.* **7**, 53-59.

Narayanasamy S., Jollivet P., Godon N., Angeli F., Gin S., Cabié M., Cambedouzou J., Le Guillou C. and Abdelouas A. (2019) Influence of composition of nuclear waste glasses on vapor phase hydration. *J. Nucl. Mater.* **525**, 53-71.

Nicoleau E., Schuller S., Angeli F., Charpentier T., Jollivet P., Le Gac A., Fournier M., Mesbah A. and Vasconcelos F. (2015) Phase separation and crystallization effects on the structure and durability of molybdenum borosilicate glass. *J. Non-Cryst. Solids* **427**, 120-133.

Nicoleau E., Angeli F., Schuller S., Charpentier T., Jollivet P. and Moskura M. (2016) Rare-earth silicate crystallization in borosilicate glasses: Effect on structural and chemical durability properties. *J. Non-Cryst. Solids* **438**, 37-48.

Nuclear Energy Agency (2018) State-of-the-art report on the progress of nuclear fuel cycle chemistry. Nuclear Science. Paris (France): OECD/NEA Publising. https://www.oecd-nea.org/jcms/pl_14970/state-of-the-art-report-on-the-progress-of-nuclear-fuel-cycle-chemistry

Ojovan M. I., Lee W. E. (2005) An introduction to nuclear waste immobilisation. Elsevier, Oxford (UK).

Ojovan M. I. and Lee W. E. (2007) New developments in glassy nuclear wasteforms. Hauppauge, New York (USA): Nova Science Publishers.

Ojovan M. I. and Lee W. E. (2010) Glassy wasteforms for nuclear waste immobilization. *Metall. Mater. Trans. A* **42**, 837-851.

Orlhac X., Fillet C. and Phalippou J. (1999) Study of crystallization mechanisms in the French nuclear waste glass. *Mat. Res. Soc. Symp. Proc.* **556**, 263-270.

Orlhac X. (1999) Study of the thermal stability of nuclear glass. Long-term evolution modeling. (In French) PhD of the University of Montpellier II (France). http://www.iaea.org/inis/collection/NCLCollectionStore/_Public/31/058/31058405.pdf.

Orlova A. I. and Ojovan M. I. (2019) Ceramic mineral waste-forms for nuclear waste immobilization. *Materials* **12**, 2638.

Pacaud F., Fillet C. and Jacquet-Francillon N. (1991) Effect of platinoids on French LWR reference glass properties. *Mat. Res. Soc. Symp. Proc.* **257**, 161-167.

Pace S., Cannillo V., Wu J., Boccaccini D. N., Seglem S. and Boccaccini A. R. (2005) Processing glass-pyrochlore composites for nuclear waste encapsulation. *J. Nucl. Mater.* **341**, 12-18.

Parruzot B., Jollivet P., Rébiscoul D. and Gin S. (2015) Long-term alteration of basaltic glass: Mechanisms and rates, *Geochim. Cosmochim. Acta.* **154**, 28-48.

Patil D. S., Konale M., Gabel M., Neill O. K., Crum J. V., Goel A., Stennett M. C., Hyatt N. C. and McCloy J. S. (2018) *J. Nucl. Mater.* **510**, 539-550.

Pegg I. L. Turning nuclear waste into glass. (2015) *Physics Today* **68**, 33-39.

Peuget S., Cachia J.-N., Jégou C., Deschanels X., Roudil D., Broudic V., Delaye J.M. and Bart J.-M. Irradiation stability of R7T7-type borosilicate glass. *J. Nucl. Mater.* **354** (2006) 1-13.

Peuget S., Broudic V., Jégou C., Frugier P., Roudil D., Deschanels X., Rabiller H. and Noel P. Y. (2007) Effect of alpha irradiation on the leaching behaviour of nuclear glass. *J. Nucl. Mater.* **362**, 474-479.

Peuget S., Delaye J.-M. and Jégou C. (2014) Specific outcomes of the research on the radiation stability of the French nuclear glass towards alpha decay accumulation. *J. Nucl. Mater.* **444**, 76-91.

Pflieger R., Malki M., Guari Y., Larionova J. and Grandjean A. (2009) Electrical conductivity of RuO_2-borosilicate glasses: Effect of the synthesis route. *J. Am. Ceram. Soc.* **92**, 1560-1566.

Piovesan V., Bardez-Giboire I., Fournier M., Frugier P., Jollivet P., Montouillout V., Pellerin N. and Gin S. (2018) Chemical durability of peraluminous glasses for nuclear waste conditioning. *npj Mater. Degrad.* **2**, 7.

Prakash A. D., Singh M., Mishra R. K., Valsala T. P., Tyagi A. K., Sarkar A. and Kaushik C. P. (2019) Studies on modified borosilicate glass for enhancement of solubility of molybdenum. *J. Non-Cryst. Solids* **510**, 172-178.

Quintas A., Caurant D., Majérus O., Dussossoy J-L. and Charpentier T. (2008) Effect of changing the rare earth cation type on the structure and crystallisation behaviour of an aluminoborosilicate glass. *Phys. Chem. Glasses: Eur. J. Glass Sci. Technol. B* **49**, 192-197.

Ren M., Deng L., and Du J. (2017). Bulk, surface structures and properties of sodium borosilicate and boroaluminosilicate nuclear waste glasses from molecular dynamics simulations. *J. Non-Cryst. Solids* **476**, 87-94.

Riley, B. J., Vienna, J. D., Strachan, D. M., McCloy, J. S. and Jerden, J. L. (2016). Materials and processes for the effective capture and immobilization of radioiodine: A review. *J. Nucl. Mater.* **470**, 307-326.

Rodríguez-Penalonga L. and Moratilla Soria B. Y. (2017) A review of the nuclear fuel cycle strategies and the spent nuclear fuel management technologies. *Energies* **10**, 1235.

Rose P. B., Woodward D. I., Ojovan M. I., Hyatt N. C. and Lee W. E. (2011) Crystallisation of a simulated borosilicate high-level waste glass produced on a full-scale vitrification line. *J. Non-Cryst. Solids* **357**, 2989-3001.

Sales B. C. and Boatner L. A. (1986) Lead-iron phosphate glass. In Lutze W. & Ewing R. C. (eds.) Radioactive waste forms for the future. pp 193-231. Elsevier Science Publishers B. V.

Santagneli S. H., de Araujo C. C., Strojek W., Eckert H., Poirier G., Ribeiro S. J. L. and Messaddeq Y. (2007) Structural studies of $NaPO_3$-MoO_3 glasses by solid-state nuclear magnetic resonance and Raman spectroscopy. *J. Phys. Chem. B* **111**, 10109-10117.

Schaller T., Stebbins J. F. and Wilding M. C. (1999) Cation clustering and formation of free oxide ions in sodium and potassium lanthanum silicate glasses: nuclear magnetic resonance and Raman spectroscopic findings. *J. Non-Cryst. Solids* **243**, 146-157.

Shiryaev A. A., Zubabichus Y. V., Stefanovsky S. V., Ptashkin A. G. and Marra J. C. (2009) XAFS of Pu and Hf LIII edge in lanthanide-borosilicate glass. *Mater. Res. Soc. Symp. Proc.* **1193**, 259-265.

Sobolev I. A., Dimitriev S. A., Lifanov F. A., Kobelev A. P., Stefanovky S. and Ojovan M. I (2005) Vitrification processes for low, intermediate radioactive and mixed wastes. *Glass Technol.* **46**, 28-35.

Sombret C. G. (1993) The vitrification of high-level wastes in France: from the lab to industrial plants. BNS/OECD-NEA Symposium on the safety of the nuclear fuel cycle Brussels: June 3-4, 1993. https://inis.iaea.org/collection/NCLCollectionStore/_Public/25/047/25047841.pdf

Stefanovsky S. V., Lebedev V. V., Ptashkin A. G., Dmitriev S. A. and Marra J. C. (2010) Cold crucible inductive melting technology - Application to vitrification and ceramization of high level and actinide wastes. *Adv. Sci. Technol.* **73**, pp 183-193.

Tan S., Ojovan M. I., Hyatt N. C. and Hand R. J. (2015) MoO_3 incorporation in magnesium aluminosilicate glasses. *J. Nucl. Mater*. **458**, 335-342.

Thien, B. M. J., Godon, N., Ballestero, A., Gin, S. and Ayral, A. (2012) The dual effect of Mg on the long-term alteration rate of AVM nuclear waste glasses. *J. Nucl. Mater*. **427**, 297–310.

Tournié A., Majérus O., Lefèvre G., Rager M.-N., Walmé S., Caurant D. and Barboux P. (2013) Impact of boron complexation by Tris buffer on the initial dissolution rate of borosilicate glasses. *J. Colloid Interface Sci.* **400**, 161-167.

Tribet M., Mir A.H., Gillet C., Jegou C., Mougnaud S., Hinks J.A., Donnelly S.E. and Peuget S. (2020) New insights about the importance of the alteration layer/glass interface. *J. Phys. Chem. C.* **124**, 10032-10044.

Vernaz E., Gin S. and Veyer C. (2012) Waste glass. *Comprehensive Nuclear Materials* **5**, 451-483.

Verney-Carron A., Gin S. and G. Libourel (2008). A fractured roman glass block altered for 1800 years in seawater: Analogy with nuclear waste glass in a deep geological repository. *Geochim. Cosmochim. Acta.* **72**, 5372–5385.

Verney-Carron A., Gin S., Frugier P. and Libourel G. (2010) Long-term modeling of alteration-transport coupling: Application to a fractured Roman glass. *Geochim. Cosmochim. Acta.* **74**, 2291-2315.

Wang L. and Liang T. (2012) Ceramics for high level radioactive waste solidification. *J. Adv. Ceram.* **1**, 194-203.

Weber W. J., Turcotte R.-P., Bunnel L. R., Roberts F. P. and Westsik J. H. (1979) Radiation effects in vitreous and devitrified simulated waste glass. In Chikalla T. D., Mendel J. E. (eds.), Ceramics in Nuclear Waste Management, National Information Service, Springfield, VA, CONF-790420. pp. 294-299.

Weber W. J. (1983) Radiation-induced swelling and amorphization in $Ca_2Nd_8(SiO_4)_6O_2$. *Radiat. Eff.* **77**, 295-308.

Weber W. J., Ewing R. C., Angell C. A., Arnold G. W., Cormack A. N., Delaye J. M., Griscom D. L., Hobbs L. W., Navrotsky A., Price D. L., Marshall Stoneham A. and Weinberg M. C. (1997). Radiation effects in glasses used for immobilization of high-level waste and plutonium disposition. *J. Mater. Res.* **12**, 1948-1978.

Weber W. J., Ewing R. C., Catlow C. R. A., de la Rubia T. D., Hobbs L. W., Kinoshita C., Matzkz Hj., Motta A. T., Nastasi M., Salje E. K. H., Vance E. R. and Zinkle S. J. (1998). Radiation effects in crystalline ceramics for the immobilization of high-level nuclear waste and plutonium. *J. Mater. Res.* **13**, 1434-1484.

Weber W. J. (2014) Radiation and thermal ageing of nuclear waste glass. *Proc. Mater. Sci.* **7**, 237-246.

Wilson P. D. (1996) The nuclear fuel cycle. From ore to waste. In Wilson P. D. (ed.) Oxford (UK): Oxford University Press.

Yang J. H., Park H-S. and Cho Y-Z. (2017) Al_2O_3-containing silver phosphate glasses as hosting matrices for radioactive iodine. *J. Nucl. Sci. Technol.* **54**, 1330-1337.

Zhang Y., Gregg D. J., Kong L., Jovanovich M. and Triani G. (2017) Zirconolite glass-ceramics for plutonium immobilization: The effects of processing redox conditions on charge compensation and durability. *J. Nucl. Mater.* **490**, 238-241.

Zhao D., Li L., Davis L. L., Weber W. J. and Ewing R.C. (2001) Gadolinium borosilicate glass-bonded Gd-silicate apatite: a glass-ceramic nuclear waste form for actinides. *Mater. Res. Soc. Symp. Proc.* **663**, 199-206.